Calcium Dynamics and Homeostasis in a Mathematical Model of the Principal Cell of the Cortical Collecting Tubule

YUANHUA TANG and JOHN L. STEPHENSON

From the Department of Physiology and Biophysics, Cornell University Medical College, New York, New York 10021

ABSTRACT Calcium (Ca) dynamics are incorporated into a mathematical model of the principal cell in the cortical collecting tubule developed earlier in Strieter et al. (1992*a*. *Am. J. Physiol.* 263:F1063–1075). The Ca components are modeled after the Othmer-Tang model for IP_3-sensitive calcium channels (1993, *in* Experimental and Theoretical Advances in Biological Pattern Formation, 295–319). There are IP_3-sensitive Ca channels and ATP-driven pumps on the membrane of the endoplasmic reticulum. Calcium enters the cell passively down its electrochemical gradient. A Ca pump and Na/Ca exchange in the basolateral membrane are responsible for the extrusion of cytoplasmic calcium. Na/Ca exchange can also operate in reverse mode to transport Ca into the cell. Regulatory effects of cytoplasmic Ca on the apical Na channels are modeled after experimental data that indicate apical Na permeability varies inversely with cytoplasmic Ca concentration. Numerical results on changes in intracellular Ca caused by decreasing NaCl in the bath and the lumen are similar to those from experiments in Bourdeau and Lau (1990. *Am. J. Physiol.* 258:F1497–1503). This match of simulation and experiment requires the synergistic action of the Na/Ca exchanger and the Ca regulated apical Na permeability. In a homogeneous medium, cytoplasmic Ca becomes oscillatory when extracellular Na is severely decreased, as observed in experiments of cultured principal cells (Koster, H., C. van Os, and R. Bindels. 1993. *Kidney Int.* 43:828–836). This essentially pathological situation arises because the hyperpolarization of membrane potential caused by Na-free medium increases Ca influx into the cell, while the Na/Ca exchanger is inactivated by the low extracellular Na and can no longer move Ca out of the cell effectively. The raising of the total amount of intracellular Ca induces oscillatory Ca movement between the cytoplasm and the endoplasmic reticulum. Ca homeostasis is investigated under the condition of severe extracellular Ca variations. As extracellular Ca is decreased, Ca regulation is greatly impaired if Ca does not regulate apical ionic transport. The simulations indicate that the Na/Ca exchanger alone has only limited regulatory capacity. The Ca regulated apical sodium or potassium permeability are essential for regulation of cytoplasmic Ca in the principal cell of the cortical collecting tubule.

INTRODUCTION

Cytoplasmic calcium (Ca) is an important second messenger in many cell types, including epithelial cells in the nephrons of mammalian kidney. In the last decade, the regulatory effect of Ca has been explored experimentally in many cell types in the nephron, including the principal cell of the cortical collecting tubule (CCT) (Windhager et al., 1991). Cytoplasmic Ca regulates the apical sodium (Na) and potassium (K) conductances (Chase and Al-Awaqti, 1993; Schlatter et al., 1993; Hirsh et al., 1993; Wang et al., 1993). These changes in conductivity, hence absorption and secretion rates of the cells, are manifested under manipulations that change cytoplasmic Ca, including changes in Na concentration in the mucosal or serosal media, hormonal application, and the application of a variety of drugs that affect the function of membrane proteins. Such a complex pattern of interactions warrants a comprehensive model that incorporates individual components into a complete picture.

Since calcium in blood and in the lumen are in the millimolar range, and cytoplasmic Ca is usually below the micromolar range, calcium enters the cytoplasm down a strong electrochemical gradient. There is some evidence suggesting the existence of apical Ca channels in the principal cell of CCT, at least in the cultured principal cells (Bindels et al., 1992). In addition, Ca

Address correspondence to Dr. John Stephenson, Department of Physiology and Biophysics, Cornell University Medical College, New York, NY 10021.

 J. GEN. PHYSIOL. © The Rockefeller University Press • 0022-1295/96/02/207/24 $2.00
Volume 107 February 1996 207–230

may enter the cell from other cation channels in the apical membrane. The principal cell needs certain mechanisms to clear this Ca accumulation, which is accomplished by the ATP-dependent Ca pump and the Na/Ca exchange located on the basolateral membrane (Gmaj and Murer, 1988; Windhager et al., 1991). The existence of basolateral Ca-ATPase in the principal cell has been demonstrated both enzymatically and immunologically (Doucet and Katz, 1982; Borke et al., 1987). The electrogenic Na/Ca exchanger has been shown to exist on the basolateral membrane of connecting tubule cells through manipulations on basolateral Na concentrations (Bourdeau and Lau, 1990; Windhager et al., 1991) and immunocytochemical localization (Bourdeau et al., 1993).

The primary store of intracellular Ca is the endoplasmic reticulum (ER) (Costanzo and Windhager, 1992). The Ca channels on the ER are known to be the inositol triphosphate (IP_3)-sensitive type (IP_3R) (Koster et al., 1993). The ER membrane also contains a Ca-ATPase that transports Ca into the ER (Moore et al., 1974; Parys et al., 1985). These results indicate that the Ca dynamics in the principal cell are similar to those of other cell types where an IP_3-sensitive Ca store exists.

A mathematical model has been proposed for CCT (Strieter et al., 1992*a*). It has been applied to study Na and K transport by the epithelium (Strieter et al., 1992*b*). Ca components are not included in the model. On the other hand, since the first publication of a kinetic model for IP_3R by De Young and Keizer (1992), several simpler kinetic models for IP_3R have been proposed, including the Othmer-Tang model (Atri et al., 1993; Othmer and Tang, 1993; Bezprozvanny and Ehrlich, 1994). These IP_3R models have been extended to study intracellular Ca dynamics in various cell types, including hepatocytes, *Xenopus* oocytes, pituitary gonatrophs, and pancreatic β cells (Keizer and De Young, 1993; Li et al., 1994; Tang and Othmer, 1994). In epithelial cells, intracellular Ca dynamics are usually coupled to transepithelial fluxes and intracellular homeostasis of many ionic species, including Ca itself. To date, no mathematical model has been developed for Ca dynamics in epithelial cell types. In this paper, we expand the model in Strieter et al. (1992*a*) to include various Ca components as modeled in Othmer and Tang (1993), with the objective of simulating experimental results that are related to cytoplasmic Ca dynamics and its relation to other electrolytes. Here the model for cytoplasmic Ca components is expanded from that in Othmer and Tang (1993) to incorporate Ca buffers in the cytoplasm and inside ER.

The model simulation reveals that the regulation of cytoplasmic Ca is mediated by the synergistic action of Ca regulated apical Na permeability and the basolateral Na/Ca exchange. This communication between the apical and basolateral membranes mediated through cytoplasmic Na and Ca provides a powerful feedback mechanism restoring cytoplasmic Ca toward its equilibrium value.

MATERIALS AND METHODS

The Model Network and Equations

Components of the model. The cortical collecting tubule epithelium with the principal cells and tight junctions is modeled after (Strieter et al., 1992*a*). A schematic diagram of the epithelium is shown in Fig. 1. In the center of the figure is the principal cell. To the left of the principal cell is the mucosal or luminal solution; and to the right the serosal or bath solution. The mem-

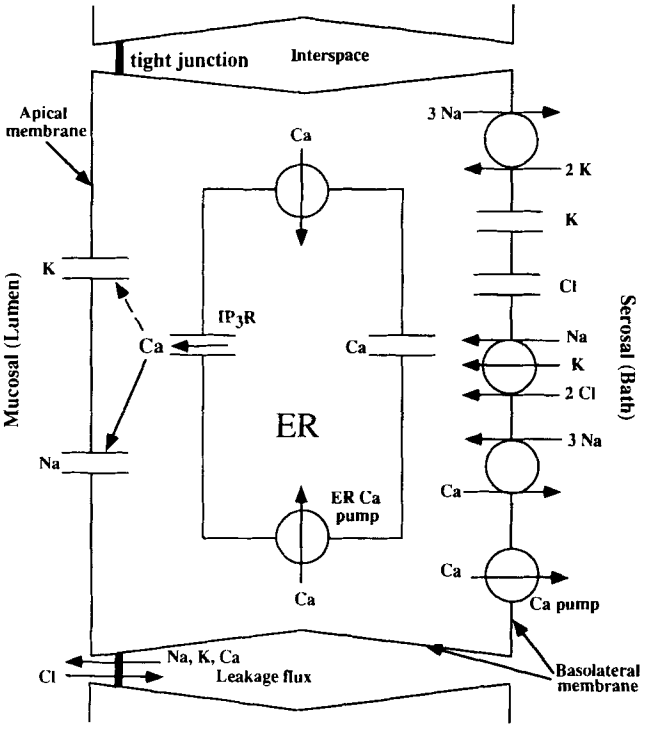

FIGURE 1. Schematic diagram of the cortical collecting tubule epithelium with the principal cell and the tight junction. The mucosal (*left*) and serosal (*right*) solutions are separated by the principal cells and the tight junctions joining the cells. The apical membrane of the cell separates the cytoplasm from the mucosal medium (also called lumen), and the basolateral membrane separates the cytoplasm and the serosal medium (also called bath). Inside the principal cell, the membrane of endoplasmic reticulum (*ER*) separates cytoplasm from the lumen of ER, which serves as an intracellular Ca store. Although all the membranes contain nonzero permeabilities to all the four ionic species, only the major conductances and transporters are shown. These include Na and K channels in the apical membrane; and K and Cl channels, Na/K and Ca pumps, a Na:K:2Cl cotransporter, and a Na/Ca exchanger in the basolateral membrane. On the ER membrane, there are a IP_3-sensitive Ca channel (*IP_3R*) for Ca release and a Ca-ATPase for pumping Ca back to the store. Electrical potential across the epithelium also drives leakage current through the tight junction.

brane of the principal cell separating the cytoplasm from the mucosal solution is the apical membrane, and that separating the cytoplasm and serosal solution is the basolateral membrane. Thus, the principal cells in CCT separate asymmetric media, with the apical side facing mucosal medium and basolateral side facing serosal medium. Tight junctions join the principal cells at the apical membrane, separating the mucosal solution from basolateral solution at cellular boundaries. They provide the diffusion barrier to volume and ionic fluxes for the small spaces between the cells. The barrier to ionic and volume fluxes in the apical and basolateral membranes of the principal cells is broken by specific membrane proteins. In the apical membrane there are Na and K channels, whereas K and chloride (Cl) channels locate on the basolateral membrane. In addition, there are active transporters located on the basolateral membrane, including Na/K pump and Ca pump, Na:K:2Cl cotransporter, and the Na/Ca exchanger. Inside the principal cell, the membrane of ER separates cytoplasm from the lumen of ER, which serves as an intracellular Ca store. On the ER membrane, there are IP_3-sensitive Ca channels for Ca release. The ER Ca-ATPase is responsible for Ca uptake and for pumping the released Ca back to the store.

It is known that there are three distinct cell types in CCT, namely, the principal cell and the α- and β-intercalated cells. The α-intercalated cell is chiefly involved in proton secretion, whereas the β-intercalated cell performs both HCO_3 secretion and Cl reabsorption. We will only model the principal cells joined together by tight junctions, since this simplification will not lose any essential components for Ca dynamics in the epithelium (Fig. 1). Thus, the system contains four compartments: the mucosal (m) and serosal (s) solutions, cytoplasmic compartment (p), and the ER (r) of the principal cell. A superscript i stands for one of the m, p, s, r compartments. The three membranes in the system, that between the principal cell and the mucosal medium, that between the principal cell and the serosal medium, and that between the cytoplasm and the ER, are denoted by superscripts ps, pm, and pr. The membrane forming the tight junction is denoted as ms (separating mucosal medium from serosal medium). Superscript ij indicates one of these membranes. In each compartment, we will consider the concentration of Na, K, Cl, Ca, and an impermeant species, denoted by C_k^i. Here the subscript k indicates the electrolyte species; k = 1, 2, 3, 4, 5 or Na, K, Cl, Ca, IMP interchangeably, corresponding to Na, K, Cl, Ca, and the impermeant species.

In addition to Ca components in the membranes, we also introduced a Na:K:2Cl cotransporter in the basolateral membrane (Fig. 1) that is not present in the Strieter et al. (1992*a*) model. The introduction of Na:K:2Cl cotransporter is to bring the concentrations of major ionic species into the physiologically observed range. The cotransporter increases the intracellular Cl concentration to ~21 mM (Rick, 1993). Without the cotransporter, the intracellular Cl will be at its electrochemical equilibrium of ~6 mM (Strieter et al., 1992*a*). To date, there are no published data that support the existence of the Na:K:2Cl cotransporter in the basolateral membrane. According to the numerical simulations of the model proposed here, some type of Cl cotransport, not necessarily Na:K:2Cl cotransport, must exist in the principal cell (such as a Na:Cl cotransporter).

Fluxes across the epithelial membranes. The fluxes across each mem-

Definition of Symbols

Subscripts	
k	ionic species, 1 (Na); 2 (K); 3(Cl); 4 (Ca); 5(IMP)
Superscripts	
i, j	compartment, p (cytoplasmic); m (mucosal); s (serosal); r (ER)
ij	membrane between compartments i and j
Independent variables	
ϕ^{ij}	membrane potential across membrane ij, mV
ϕ^{p}	membrane potential of the principal cell in culture, mV
B^i	free Ca buffer concentration in compartment i, mM
C_k^i	concentration of species k in compartment i, mM
R_{ICC}	proportion IP_3R in the inhibited state, dimensionless
V	volume of the principal cells, cm^3 per cm^2 epithelium (cm^3/cm^2 ep.)
Dependent variables	
μ_k^{ij}	electrochemical potential difference of species k across membrane ij, $J \cdot mmol^{-1}$
CaB^i	buffered Ca in compartment i, mM
$\bar{C}_k^{ij}$	mean membrane concentration of species k in membrane ij, mM
R	proportion of (IP_3R) in the bare receptor state, dimensionless
R_1	proportion IP_3R in the IP_3-bound state, dimensionless
R_{1C}	proportion IP_3R in the IP_3- and positive Ca-bound state, dimensionless
V^p	volume of the cytoplasm, cm^3/cm^2 ep.
V^r	volume of the ER, cm^3/cm^2 ep.
Fluxes	
J_{CaP}^{pr}	Ca flux across the ER membrane by the Ca-ATPase, $\mu M/s \cdot cm^2$ ep.
J_{CaP}^{ps}	Ca flux across the basolateral membrane carried by Ca pump, $mmol/s \cdot cm^2$ ep.
J_{ch}^{rp}	Ca flux across the ER membrane through IP_3R, $\mu M/s \cdot cm^2$ ep.
J_K^{act}	K flux carried by the Na/K pump across the basolateral membrane, $mmol/s \cdot cm^2$ ep.
J_k^{ij}	ionic flux of k species across membrane ij, $mmol/s \cdot cm^2$ ep.
J_k^{cotr}	flux of species k carried by the Na:K:2Cl cotransporter, $mmol/s \cdot cm^2$ ep.

(continued on next page)

(continued from previous page)

J^{rp}_{leak}	Ca leak flux across the ER membrane, μM/s·cm² ep.
J^{act}_{Na}	Na flux of Na/K pump across the basolateral membrane, mmol/s·cm² ep.
$J^{ps}_{Na/Ca,Ca}$	Ca flux carried by Na/Ca exchange, mmol/s·cm² ep.
$J^{ps}_{Na/Ca,Na}$	Na flux carried by Na/Ca exchange, mmol/s·cm² ep.
J^{ij}_{v}	volume flux across membrane ij, cm³/s·cm² ep.
Constants	
F	Faraday constant, coulombs/mmol
R	universal gas constant, J·mmol^{-1}·K^{-1}
T	absolute temperature in kelvins, K
z_k	valence of species k
Kinetic constant	
b_1	binding rate of Ca to cytoplasmic buffers, (μM·s)$^{-1}$
b_2	binding rate of Ca to ER buffers, (μM·s)$^{-1}$
b_{-1}	unbinding rate of Ca from cytoplasmic buffers, s^{-1}
b_{-2}	unbinding rate of Ca from ER buffers, s^{-1}
$J^{pr}_{max,Ca}$	maximal Ca flux across the ER membrane by Ca pump, μM/s·cm² ep.
$J^{ps}_{max,Ca}$	maximal Ca flux across ps membrane by Ca pump, mmol/s·cm² ep.
$J^{ps}_{max,Na}$	maximal rate of Na/K pump across ps membrane, mmol/s·cm² ep.
$J^{ps}_{sc,Na/Ca}$	scaling Ca flux across ps membrane carried by the Na/Ca exchanger, mmol/s·cm² ep.
K_i	dissociation constant of IP_3 (i = 1) and positive regulatory Ca (i = 2) to IP_3R, s^{-1}
$K^{pr}_{M,Ca}$	Michaelis-Menten constant for Ca flux across the ER membrane by the Ca-ATPase, μM
$K^{ps}_{M,Ca}$	Michaelis-Menten constant of Ca pump on the basolateral membrane, μM
$K^{ps}_{M,K}$	Michaelis-Menten constant for Na/K pump across the basolateral membrane, mM
$K^{ps}_{M,Na}$	Michaelis-Menten constant for Na/K pump across the basolateral membrane, mM
k_3	binding constant of negative regulatory Ca to IP_3R, μM^{-1} s^{-1}
k_{-3}	unbinding constant of negative regulatory Ca from IP_3R, s^{-1}
Membrane parameters	
A^{ij}	membrane area of membrane ij, cm²/cm² ep.
C^{ij}_{q}	electrical capacitance of membrane ij, μF/cm²
L^{ij}_{v}	hydraulic water permeability across membrane ij, cm³/s·mmHg·cm² ep.
P^{pr}_{ch}	coefficient for Ca conductance from IP_3R, 1/s·cm² ep.
P^{pr}_{leak}	leakage coefficient for the ER membrane to Ca, 1/s·cm² ep.
P^{ij}_{k}	Goldman permeability coefficient of species k across membrane ij, cm³/s·cm² ep.
σ^{ij}_{k}	reflection coefficient of species k across membrane ij, dimensionless
Other parameters	
$[B^i]_T$	total Ca buffers in compartment i (i = 1 (cytoplasm), 2 (ER)), mM
I	concentration of IP_3 in the cytoplasm, μM
$K_{Na,Ca}$	constant for the switching point on the regulation of P^{pm}_{Na} by Ca, mM
$K_{K,Ca}$	constant for the switching point on the regulation of P^{pm}_{K} by Ca, mM
v_r	volume ratio of the ER to the cytoplasm, dimensionless

brane are composed of two parts, volume fluxes carried by water, denoted by J^{ij}_v , and ionic fluxes, denoted by J^{ij}_k . We will use the convention $J^{ij} = -J^{ji}$ for either volume or solute flux, with the positive direction from compartment i to compartment j.

J^{ij}_v is determined by the osmotic gradient across the membrane ij and the membrane permeability to water.

$$J^{ij}_v = L^{ij}_v RT\left(C^j_5 - C^i_5 + \sum_{k=1}^{4} \sigma^{ij}_k \left[C^j_k - C^i_k \right] \right), \tag{1}$$

where L^{ij}_v is its hydraulic water permeability, and σ^{ij}_k the reflection coefficient of species k. RT is the product of gas constant (R) and absolute temperature (T). We do not have a term for intracellular pressure for the principal cell as in Strieter et al. (1990), which means that the only driving force for volume flux is the osmolality difference. At equilibrium, the osmolalities of different compartments are the same.

The electrolyte flux, J^{ij}_k , is composed of a convective term, a passive conducting term, and an active transport term. The convective term and the passive conducting term due to electrochemical gradients across each membrane are modeled by the Goldman constant field equation (Goldman, 1943).

$$J^{ij}_k = \begin{cases} (1 - \sigma^{ij}_k)\,\bar{C}^{ij}_k J^{ij}_v + \dfrac{P^{ij}_k Z_k F \phi^{ij}}{RT} \dfrac{C^j_k - C^i_k \exp\left(\dfrac{-z_k F \phi^{ij}}{RT}\right)}{1 - \exp\left(\dfrac{-z_k F \phi^{ij}}{RT}\right)} \\ \qquad + J^{act}_k, \text{ if } |\phi^{ij}| > 0 \\ (1 - \sigma^{ij}_k)\,\bar{C}^{ij}_k J^{ij}_v + P^{ij}_k (C^j_k - C^i_k) + J^{act}_k, \quad \text{if } |\phi^{ij}| = 0, \end{cases} \tag{2}$$

where $[z_1, z_2, z_3, z_4] = [1, 1, -1, 2]$ are the valences for corresponding ions; ϕ^{ij} the electrical potential across the membrane ij. Numerically, we use $\epsilon = 1.0 \times 10^{-6}$ mV as the switching value be-

tween the two expressions of Eq. 2. $\bar{C}_k^{ij}$ is the mean concentration of species k (page 61 in Schultz, 1980),

$$\bar{C}_k^{ij} = \frac{C_k^j - C_k^i}{lnC_k^j - lnC_k^i}. \tag{3}$$

The active transport ionic fluxes are determined by various pumps and transporters shown in Fig. 1. For the Na/K pump on the basolateral membrane, we use the model developed by Hoffman and Tosteson (1971), which was also used in Strieter et al. (1992*a*).

$$J_{Na}^{act} = J_{max,Na}^{ps}\left(\frac{C_{Na}^p}{C_{Na}^p + K_{M,Na}^{ps}}\right)^3\left(\frac{C_K^s}{C_K^s + K_{M,K}^{ps}}\right)^2. \tag{4}$$

Due to the 3:2 stoichiometry of the Na/K pump, the active transport of K is in the opposite direction:

$$J_K^{act} = -\frac{2}{3}J_{Na}^{act}. \tag{5}$$

The variable affinities of the Na and K binding sites in the principal site and the serosal side of the membrane are modeled after Garay and Strieter (Garay and Garrahan, 1973; Strieter et al., 1990).

$$K_{M,Na}^{ps} = 0.2\left(1 + \frac{C_K^p}{8.33}\right), \qquad K_{M,K}^{ps} = 0.1\left(1 + \frac{C_{Na}^s}{18.5}\right). \tag{6}$$

The basolateral cotransporter for Na, K, Cl is modeled by a nonequilibrium thermodynamics model with only one specific parameter, the cotransport coefficient, as in Strieter et al. (1990):

$$\begin{bmatrix} J_{Na}^{cotr} \\ J_K^{cotr} \\ J_{Cl}^{cotr} \end{bmatrix} = L^{cotr}\begin{bmatrix} 1 & 1 & 2 \\ 1 & 1 & 2 \\ 2 & 2 & 4 \end{bmatrix}\begin{bmatrix} \mu_{Na}^{ps} \\ \mu_K^{ps} \\ \mu_{Cl}^{ps} \end{bmatrix}. \tag{7}$$

The electrochemical potential of each ion is given by

$$\mu_k^{ps} = RTln\,(C_k^p/C_k^s) + z_kF\phi^{ps}, \qquad k = 1,2,3. \tag{8}$$

For the ATP-driven Ca pump on the basolateral membrane, the rate is described by a Michaelis-Menten form with Hill coefficient 2, as given in Haynes and Mandveno (1987).

$$J_{CaP}^{ps} = J_{max,Ca}^{ps}\frac{(C_{Ca}^p)^2}{(C_{Ca}^p)^2 + (K_{M,Ca}^{ps})^2} \tag{9}$$

The Na/Ca exchange is modeled after Campbell et al. (1988) with 3:1 stoichiometry for Na vs Ca. The driving forces for the exchange are the chemical concentration gradients of Na and Ca and the membrane potential across the ps membrane. Depending on the concentration gradient of Na and Ca and the membrane potential across the ps membrane, the exchanger can function in two different directions: one is to transport one Ca outward from the cytoplasm to the serosal medium in exchange for three Na entering the cell; and the other is to transport three Na outward from the cell in exchange for one Ca entering the cell. The Ca flux carried by this exchange is given by

$$J_{Na/Ca,Ca}^{ps} = J_{sc,Na/Ca}^{ps} \cdot \frac{(C_{Na}^s)^3 C_{Ca}^p \exp(-F\phi^{ps}/2RT) - (C_{Na}^p)^3 C_{Ca}^s \exp(F\phi^{ps}/2RT)}{1 + 0.0095\,[C_{Ca}^p\,(C_{Na}^s)^3 + C_{Ca}^s\,(C_{Na}^p)^3]}, \tag{10}$$

with $J_{Na/Ca,Na}^{ps} = -3J_{Na/Ca,Ca}^{ps}$. The numerator of Eq. 10 reflects the driving force for the exchange determined by the electrochemical gradients for species involved and the specific stoichiometry of the exchange, and the denominator represents an empirical term for the saturation of the exchanger obtained for the Na/Ca exchanger of cardiac type (Campbell et al., 1988). $J_{sc,Na/Ca}^{ps}$ is the scaling factor for Ca flux carried by the exchanger. Fig. 2 shows the Ca flux generated by this exchange under varying conditions of intracellular, extracellular Na and Ca concentrations, and the basolateral membrane potential. In contrast to Ca-ATPase, $J_{Na/Ca,Ca}^{ps}$ saturates at a much higher C_{Ca}^p.

The parameter values used for the fluxes across the apical and the basolateral membranes are listed in Table I. Most of the parameter values are adopted directly from Strieter et al. (1992*a*), with minor adjustments. For the Ca components, we estimate P_{Ca}^{pm} based on the observed Ca absorption rate reported in Bindels et al. (1992) and Magaldi et al. (1989). $K_{M,Ca}^{ps}$ for the Ca-ATPase in the cortex of kidney is reported in Gmaj and Murer (1988) to be ~0.14 μM. We use 0.1 μM in our model. The value for the maximal rate of pumping $J_{max,Ca}^{ps}$ is estimated such that C_{Ca}^p is around 100 nM. Estimation of $J_{sc,Na/Ca}^{ps}$ is based on the behavior of the cell under variations in C_{NaCl}^s (Bourdeau and Lau, 1990; Koster et al., 1993).

Intracellular Ca fluxes and buffering. In our model, the endoplasmic reticulum is considered to be uniformly distributed in the whole cytoplasm, e.g., a continuum yet only occupying a portion

TABLE I

Parameter Definitions and Values for the Apical and Basolateral Membranes

Definition	pm	ps	ms
		cm^2/cm^2 ep.	
Area	1.46	12.25	0.001
		$cm^3/s \cdot mmHg \cdot cm^2$ ep.	
Lv	3.0×10^{-3}	8.1×10^{-2}	3.0×10^{-4}
σ_k, k = 1, ..., 4	1.0	1.0	1.0
		$cm^3/s \cdot cm^2$ ep.	
P_k			
NA	1.36×10^{-6}	1.2×10^{-8}	1.2×10^{-6}
K	1.12×10^{-5}	1.0×10^{-5}	2.0×10^{-6}
Cl	1.5×10^{-9}	1.0×10^{-6}	1.6×10^{-7}
Ca	1.8×10^{-7}	1.0×10^{-9}	5.0×10^{-8}
		$pmol/s \cdot cm^2$ ep.	
Active transporters			
$J_{max,Na}^{ps}$		2.4×10^3	
$J_{max,Ca}^{ps}$		1.9	
$J_{sc,Na/Ca}^{ps}$		7.0×10^{-2}	
		$mmol^2/J \cdot s \cdot cm^2$ ep.	
Na:K:2Cl cotransport coefficient			
L^{cotr}		4.0×10^{-6}	
Michaelis-Menten constant			
$K_{M,Ca}^{ps}$		0.075 μM	

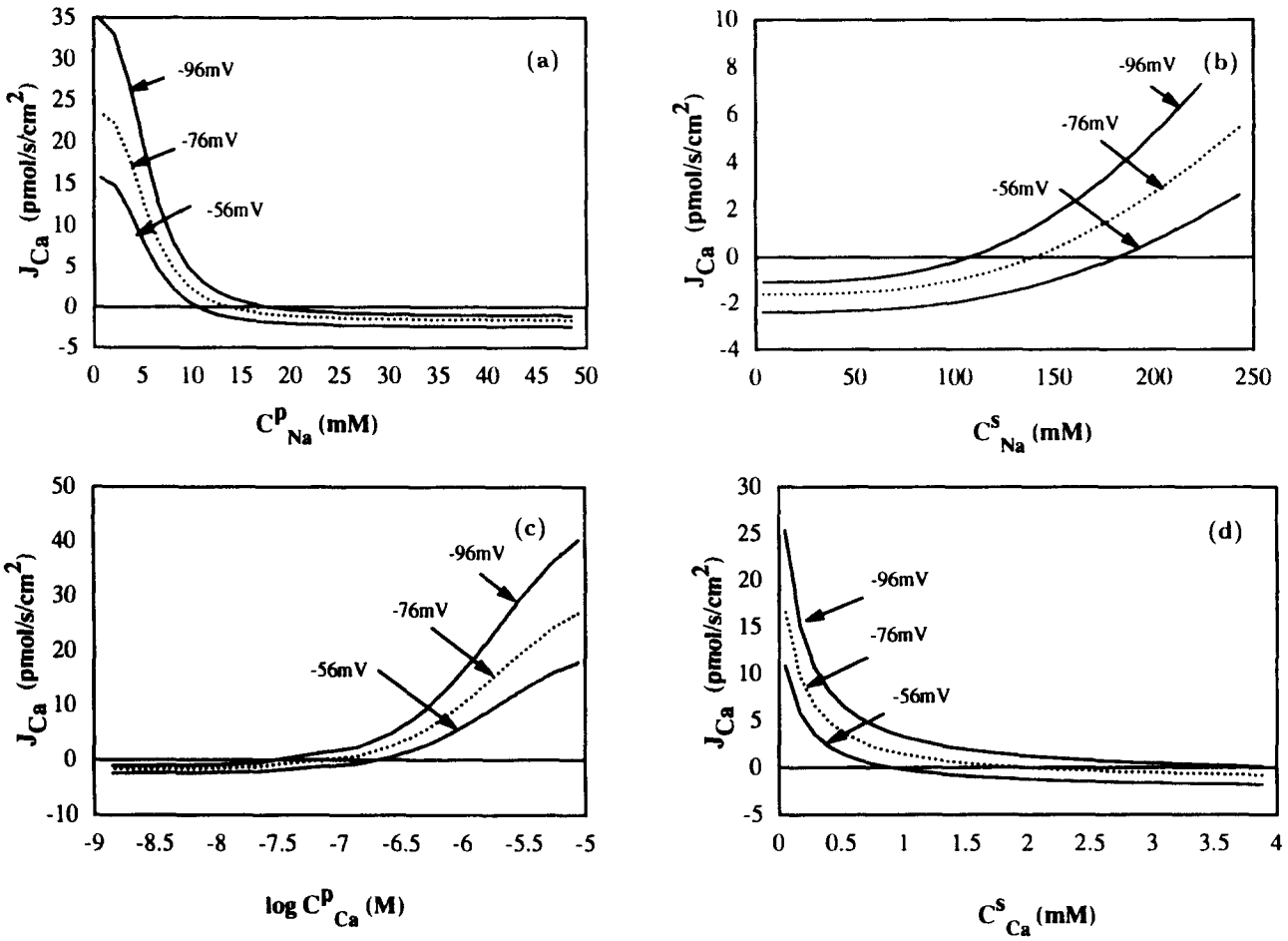

FIGURE 2. Ca flux across the basolateral membrane carried by the Na/Ca exchange as each of the controlling factors (membrane potential, Na and Ca concentrations in the cytoplasm and in the bath) is individually varied. (*a*) Varying C^p_{Na} only; (*b*) varying C^s_{Na} only; (*c*) varying C^p_{Ca} only; and (*d*) varying C^s_{Ca} only. The other controlling factors in each panel are at fixed values given in Table III.

of the complete volume. The ER serves as the Ca store, and its membrane contains the IP_3-sensitive Ca channels. The volume of the ER relative to that of the cytoplasm is assumed to be at a fixed ratio of $\nu_r = V^r/V^p$. As the cell volume changes, both the volume of the cytoplasm and the volume of the ER change proportionally so that ν_r remains a constant.

IP_3R is a hetero-tetramer that includes at least two different subtypes (Yamamoto-Hino et al., 1994). This channel is up-regulated by cytoplasmic IP_3. Cytoplasmic Ca can both potentiate or inhibit the channel opening, depending on its concentration. The time scales of the interaction for the potentiating effect and the inhibitory effect also differs. De Young and Keizer first propose a kinetic scheme for these aspects of channel regulation (De Young and Keizer, 1992). They successfully showed that their model can explain many aspects of Ca dynamics, including excitability, Ca oscillations, and the highly elevated cytoplasmic Ca levels at over-stimulated cases (Keizer and De Young, 1993; Li et al., 1994). Since the publication of the De Young-Keizer model, several simplified models have appeared. Here, we use a four-state model for the IP_3R Ca channel proposed by Othmer and Tang (1993). The transitions between the different states occur according to the following sequential scheme.

$$
\begin{aligned}
R + I &\underset{k_{-1}}{\overset{k_1}{\rightleftarrows}} R_I, \\
R_I + C &\underset{k_{-2}}{\overset{k_2}{\rightleftarrows}} R_{IC^+}, \\
R_{IC^+} + C &\underset{k_{-3}}{\overset{k_3}{\rightleftarrows}} R_{IC+C^-}.
\end{aligned}
\tag{11}
$$

Here R denotes the bare receptor for the IP_3-sensitive Ca channel, I denote IP_3, and C the cytoplasmic Ca. Superscripts + and − on C denote the association of Ca to the positive or negative regulatory site on the receptor. Therefore, R_I is the IP_3R with IP_3 bound to it, R_{IC^+} the IP_3R with IP_3 bound to its site and a Ca bound to the positive regulatory site, and $R_{IC^+C^-}$ the IP_3R with all the regulatory sites occupied. R and R_I are the activatable states, R_{IC^+} the activated state, and $R_{IC^+C^-}$ the inhibited state.

Among various schemes proposed for the kinetics of IP_3R, this scheme is the simplest, i.e., including the least number of param-

eters and channel states (De Young and Keizer, 1992; Atri et al., 1993; Bezprozvanny and Ehrlich, 1994). It addresses adequately the effect of IP_3 and Ca on the receptor and simulates the experimental data well (Tang et al., 1995). Although it is known that the subunit in the channel complex interact cooperatively (Watras et al., 1991), its exact nature of cooperativity is still unclear. Previous theoretical and numerical studies on this issue in Tang (1993) are inconclusive. The model used here simply assumes that each subunit functions independently in response to IP_3 and Ca changes. Although this approach cannot address the regulation of channel events at a single receptor level, it is adequate in explaining experimental data for a population of receptors (Bezprozvanny and Ehrlich, 1994).

Let R, R_I, R_{IC}, and R_{ICC} denote the fractions in states R, R_I, R_{IC^+}, and $R_{IC^+C^-}$, respectively, and I for cytoplasmic IP_3 concentration. Then the governing equations for the channel fractions are as follows (Othmer and Tang, 1993).

$$\begin{aligned}
\frac{dR}{dt} &= k_1 I \cdot R + k_{-1} R_I, \\
\frac{dR_I}{dt} &= -(k_{-1} + k_2 C_{Ca}^p) R_I + k_1 I \cdot R + k_{-2} R_{IC}, \\
\frac{dR_{IC}}{dt} &= -(k_{-2} + k_3 C_{Ca}^p) R_{IC} + k_2 C_{Ca}^p \cdot R_I + k_{-3} R_{ICC}, \\
\frac{dR_{ICC}}{dt} &= k_3 C_{Ca}^p \cdot R_{IC} - k_{-3} R_{ICC}.
\end{aligned} \tag{12}$$

We assume that the binding of IP_3 and the positive regulatory Ca to the IP_3R obey fast dynamics, so that approximately,

$$\frac{dR}{dt} = \frac{dR_I}{dt} = 0.$$

By using the fact that $R + R_I + R_{IC} + R_{ICC} = 1$, we get

$$\begin{aligned}
R &= \frac{K_2 (1 - R_{ICC}) K_1 / I}{C_{Ca}^p + K_2 (1 + K_1 / I)}, \\
R_I &= \frac{K_2 (1 - R_{ICC})}{C_{Ca}^p + K_2 (1 + K_1 / I)}, \\
R_{IC} &= \frac{C_{Ca}^p (1 - R_{ICC})}{C_{Ca}^p + K_2 (1 + K_1 / I)},
\end{aligned} \tag{13}$$

where $K_i = k_{-i}/k_i$, (i = 1,2), are the dissociation constants for each binding/unbinding step. Hence the governing equations for the IP_3-sensitive channel reduce to:

$$\frac{dR_{ICC}}{dt} = -k_{-3} R_{ICC} + \frac{k_3 (C_{Ca}^p)^2 (1 - R_{ICC})}{C_{Ca}^p + K_2 (1 + K_1 / I)}. \tag{14}$$

This single gating equation for the channel dynamics and the algebraic equation for the open channel, R_{IC}, in Eq. 13 will be the only equations used in the comprehensive model. The Ca conductance across the IP_3-sensitive channel is modeled as a linear function of the channel fraction in the R_{IC^+} state multiplied by the Ca gradient across the ER membrane (De Young and Keizer, 1992; Othmer and Tang, 1993).

$$J_{ch}^{rp} = P_{ch}^{rp} \cdot \frac{C_{Ca}^p (1 - R_{ICC})}{C_{Ca}^p + K_2 (1 + K_1 / I)} (C_{Ca}^r - C_{Ca}^p). \tag{15}$$

In addition to the Ca channel conductance, we assume that there is a leakage of Ca from the ER into the cytoplasm, and it is depicted simply by a linear rate driven by the Ca gradient across the ER membrane (Othmer and Tang, 1993).

$$J_{leak}^{rp} = P_{leak}^{rp} (C_{Ca}^r - C_{Ca}^p). \tag{16}$$

The Ca pump on the ER membrane is modeled similarly to the Ca pump on the basolateral membrane (Gmaj and Murer, 1988; De Young and Keizer, 1992), i.e.,

$$J_{CaP}^{pr} = \frac{J_{max,Ca}^{pr} (C_{Ca}^p)^2}{(C_{Ca}^p)^2 + (K_{M,Ca}^{pr})^2}. \tag{17}$$

The combined Ca flux across the membrane of rp is

$$J_{Ca}^{rp} = J_{leak}^{rp} + J_{ch}^{rp} - J_{CaP}^{pr}. \tag{18}$$

In addition to the fluxes across the three distinct membranes, there are internal biochemical processes that modify Ca concentration in the two compartments. Ca in the cytoplasm can bind with polyvalent anions, proteins, and fluorescent dyes once they have entered the cell. It is also certain that there are Ca binding molecules inside the ER that buffer Ca. For simplicity, we model the various buffers by assuming a single kinetics for the combined effects from these buffers. Namely, we assume

$$\begin{aligned}
C_{Ca}^p + B^p &\underset{b_{-1}}{\overset{b_1}{\rightleftarrows}} CaB^p, \\
C_{Ca}^r + B^r &\underset{b_{-2}}{\overset{b_2}{\rightleftarrows}} CaB^r,
\end{aligned} \tag{19}$$

where B^p and B^r are for the free buffers in the compartments of the cytoplasm and the ER. The total amount of buffers in the cytoplasm will be denoted $[B^p]_T$, and that in the ER $[B^r]_T$. Since the total amount of buffer in each compartment is conserved, we have $[B^p]_T = B^p + CaB^p$ and $[B^r]_T = B^r + CaB^r$.

Parameter values for the IP_3R kinetics and other components are based on Othmer and Tang (1993). For Ca buffering in the cytoplasm and in the ER, we assume that they are fast processes compared with the physiological processes we study (Robertson et al., 1987; Luo and Rudy, 1994). The majority of Ca in the cytoplasm and in the ER is in the buffered form. There are no reports on typical Ca buffer concentrations for epithelial cells. In the axoplasm of *Myxicola*, typical Ca buffer concentration is estimated to be 100–200 μM in Abercrombie and Al-Baldawi (1990), with dissociation constants of 5–10 μM. The axoplasm buffer capacity, defined as,

$$\left(\frac{\text{buffered Ca}}{\text{free Ca}} \right),$$

nevertheless, can vary from 0–20 for some and 100–150 for the others, suggesting considerable axon-axon difference (Al-Baldawi and Abercrombie, 1995). In the bovine adrenal chromaffin cells, the average Ca binding capacity is 9 ± 7 for the poorly mobile component and 31 ± 10 for the fixed component, with the dissociation constants higher than 3 μM (Zhou and Neher, 1993; Wagner and Keizer, 1994). For the Ca buffers inside the

ER, no direct measurements of the buffer concentrations and their dissociation constants are available in the literature. Secondary evidence suggests the total buffer concentration to be somewhere from hundreds of micromolar to millimolar range, while the free Ca concentration is in the range 1−100 μM (personal communications) (Milner et al., 1992; Kendall et al., 1994). In our model, the concentration of Ca buffers in the cytoplasm is assumed to be 120 μM and that inside the ER is 1.2 mM. The dissociation constant K_d for the cytoplasmic buffer is 6.67 μM and for the ER buffer 50 μM. The parameter values for the intracellular Ca fluxes and reactions are listed in Table II.

The comprehensive model. To develop a comprehensive model of the principal cell-tight junction complex under the open circuit condition, we assume the serosal potential to be the ground potential. The independent variables for the system are the membrane potential of the principal cell (ϕ^{ps}), the potential across the apical membrane (ϕ^{pm}), the cell volume (V), the electrolyte concentrations (C^{p}_{k}, k = 1, . . ., 4), Ca inside ER (C^{r}_{Ca}), the Ca channel state R_{IC+C^-} (R_{ICC}), and the free Ca buffer concentration in both the cytoplasm and the ER (B^p and B^r). The total number of the system unknowns is 11. The dependent variables include C^{p}_{IMP}, the electrical potential across the epithelium $\phi^{ms} = -\phi^{pm} + \phi^{ps}$, volume of the cytoplasm and ER (V^p and V^r), channel states of IP_3R other than R_{ICC} (R, R_I, R_{IC}), and the buffered Ca in the cytoplasm and inside the ER (CaB^p and CaB^r).

The ionic composition of the ER and the transport of ionic species other than Ca across the ER membrane are not clear experimentally. It is also uncertain if there is a membrane potential across the ER membrane, but most likely not, since the ER membrane is relatively permeable to ionic species such as Na and K. If there is an ER membrane potential, this membrane potential will affect the Ca release through the IP_3R. In this model, we do not have the ionic concentrations for Na, K, Cl and impermeant species in the ER as independent variables. Instead, we assume that the ER membrane is permeable to Na, K, and Cl, thus there is no membrane potential across the ER membrane. To maintain the electroneutrality of ER, we assume that as Ca is released, the charge carried by it is balanced by the secondary currents of Cl and K (or Na). In addition, we assume that as Ca is released, the osmolality of the ER does not change. This is accomplished by balancing the release of Ca to the release of Cl and the uptake of K (Na). These requirements are fulfilled by the cotransport of 2Ca (release) to 1 Cl (release) and 3 K (uptake).

In addition to the channel gating equation for IP_3R (Eq. 14), the other system equations are obtained from conservation for the electrical charge (ϕ^{pm}, ϕ^{ps}), the combined volume of cytoplasm-ER complex (V), and the mass of each electrolyte (C^{p}_{Na}, C^{p}_{K}, C^{p}_{Cl}, C^{p}_{Ca}, and C^{r}_{Ca}). Let us assume that the electrical capacitances for the two membranes are C^{pm}_{q} and C^{ps}_{q}, which are fixed constants determined by the surface areas of the two membranes, and the electrical capacitance of tight junction is 0. The ionic currents are computed for different apical and basolateral membrane surface area, A^{pm} and A^{ps}, in the unit of cm^2 ep. (shorthand for $cm^2 \cdot$ epithelium). The actual cell membrane is ~10,000 times smaller than this value. The specific membrane capacity is set at 1 μF/cm^2 (Luo and Rudy, 1994). Therefore, $C^{ij}_{q} = A^{ij}$ (μF). The system equations are:

$$
\begin{aligned}
C^{pm}_{q}\frac{d\phi^{pm}}{dt} &= -\sum_{k=1}^{4} z_k F(J^{pm}_{k} + J^{ms}_{k}),\\
C^{ps}_{q}\frac{d\phi^{ps}}{dt} &= -\sum_{k=1}^{4} z_k F(J^{ps}_{k} - J^{ms}_{k}),\\
\frac{dV}{dt} &= -J^{ps}_{v} - J^{pm}_{v},\\
\frac{d(V^p \cdot C^{p}_{Na})}{dt} &= -J^{ps}_{Na} - J^{pm}_{Na},\\
\frac{d(V^p \cdot C^{p}_{K})}{dt} &= -J^{ps}_{K} - J^{pm}_{K} - 1.5\,V^r J^{rp}_{Ca},\\
\frac{d(V^p \cdot C^{p}_{Cl})}{dt} &= -J^{ps}_{Cl} - J^{pm}_{Cl} + 0.5\,V^r J^{rp}_{Ca},\\
\frac{d(V^p \cdot C^{p}_{Ca})}{dt} &= -J^{ps}_{Ca} - J^{pm}_{Ca}\\
&\quad + V^r J^{rp}_{Ca} - b_1 V^p C^{p}_{Ca} B^p + b_{-1} V^p([B^p]_T - B^p),\\
\frac{d(V^r \cdot C^{r}_{Ca})}{dt} &= -V^r J^{rp}_{Ca} - b_2 V^r C^{r}_{Ca} B^r + b_{-2} V^r([B^r]_T - B^r),\\
\frac{d(V^p \cdot B^p)}{dt} &= -b_1 V^p C^{p}_{Ca} B^p + b_{-1} V^p([B^p]_T - B^p),\\
\frac{d(V^r \cdot B^r)}{dt} &= -b_2 V^r C^{r}_{Ca} B^r + b_{-2} V^r([B^r]_T - B^r),\\
\frac{dR_{ICC}}{dt} &= k_3 (C^{p}_{Ca})^2 \frac{(1.0 - R_{ICC})}{K_2(K_1/I + 1.0) + C^{p}_{Ca}} - k_3 R_{ICC},
\end{aligned}
\tag{20}
$$

where V^p stands for the volume of cytoplasm, and V^r the volume of ER, with $V^p + V^r = V$ and $V^r/V^p = \nu_r$. The reader should refer to **Definition of Symbols** for the usage of symbols in this equation.

We follow the data in Silver et al. (1993) and in Frindt et al. (1993) to model the regulation of C^{p}_{Ca} on P^{pm}_{Na}. Because the channel opening or closing in response to C^{p}_{Ca} increasing or decreasing cannot be fitted by a single exponential curve, we choose a curve of two exponentials, namely,

$$
P^{pm}_{Na} = \begin{cases} P^{pm}_{Na,0}\exp^{-14(C_{Ca} - K_{Na,Ca}) \times 10^3} + 0.1\ P^{pm}_{Na,0} & \text{if } C_{Ca} < K_{Na,Ca} \\ P^{pm}_{Na,0}\exp^{-4.024 C_{Ca} - K_{Na,Ca} \times 10^3} + 0.1\ P^{pm}_{Na,0} & \text{otherwise,} \end{cases}
\tag{21}
$$

where $P^{pm}_{Na,0}$ is the P^{pm}_{Na} value given in Table I, and $K_{Na,Ca}$ = 150 nM. A basal leakage rate without any apical Na channel is assumed at 0.1 P_0. Although the evidence for Ca inhibition on P^{pm}_{Na}

TABLE II

Parameter Values for Intracellular Ca Handling

Parameter	Value	Parameter	Value
K_1	0.667 μM	K_2	0.126 μM
k_3	0.04 (μM · s)$^{-1}$	k_{-3}	0.021 s^{-1}
b_1	0.03 (μM · s)$^{-1}$	b_{-1}	0.2 s^{-1}
b_2	0.005 (μM · s)$^{-1}$	b_{-2}	0.25 s^{-1}
J^{max}_{pr}	1.5×10^{-2} μM/s · cm^2 ep.	$K^{pr}_{M,Ca}$	0.1 μM
P^{rp}_{ch}	1.2/s · cm^2 ep.	ν_r	0.185
P^{rp}_{leak}	0.1/s · cm^2 ep.	I	0.1 μM
$[B^p]_T$	120 μM	$[B^r]_T$	1.2 μM

as C^{p}_{Ca} increases is well established, that a decrease in C^{p}_{Ca} increases P^{pm}_{Na} is still controversial. This issue will be addressed in more detail later. The dependence of P^{pm}_{Na} on C^{p}_{Ca} is depicted in Fig. 3.

Numerical Implementation

The system equation (20) has 11 independent variables and 11 differential equations. Thus it can be solved numerically as an initial value problem. The solute concentrations in the mucosal and serosal compartments, C^{i}_{k} (i = m,s), have to be given over the time period of simulation, as well as the initial value of C^{p}_{IMP}. To obtain an equilibrium solution of the system, the initial values for the independent variables can be chosen arbitrarily.

Previous mathematical models for epithelial cells use the assumption of electrical neutrality to determine the membrane potentials (Strieter et al., 1990). This assumption, which is an approximation, corresponds to selecting $C^{ij}_{q} = 0$ in our model approach. Modeling electrical potential equations directly gives rise to a stiff system where the scale of the equations varies greatly. In addition, the differences in the concentrations of intracellular ions are significant. For example, in cytoplasm, Ca is in the μM range, while Na, Cl, and K are in the mM range. Special computational precaution is required to solve this system.

To address these issues, we use the GEAR drive subroutine developed by Hindmarsh (1974), which is specifically designed for stiff systems. We use a uniform controlled error of 1.0×10^{-5} for each discrete equation. Time steps of adaptive length are used such that each call to the subroutine gives a converged solution. We have run our program on SUN and Silicon Graphics work stations and on the IBM RISC 6000. For simulating an experiment of 20 min, the program completes within two minutes on all of these machines.

RESULTS

Steady State Solution

Open-circuit epithelium. Table III shows the solution to the open-circuit epithelium in isotonic media with the inclusion of the Na:K:2Cl cotransporter and the Ca regulatory effect on apical Na conductance.

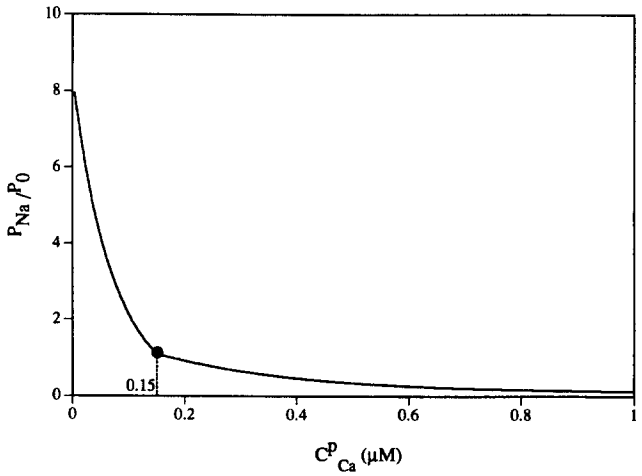

FIGURE 3. The effect of C^{p}_{Ca} on the permeability of the apical Na channel. This figure is based on the observed inhibitory effect of C^{p}_{Ca} on the apical Na channel reported in Palmer and Frindt (1987). See text for more detail.

According to this model, the principal cells actively absorb Na, while secreting K at a smaller rate. The difference in the Na absorption rate and that of secretion of K gives rise to a net positive current entering the epithelium from the apical membrane of the principal cell. This positive current is balanced by a net negative current across the tight junction, carried mainly by currents of Na, K, and Cl. Across the tight junction, Na leaks back into the lumen, and Cl is absorbed into the serosal medium due to the lumen-negative potential. K is also secreted across the tight junction. The tight junction is quite tight in the sense that the leak Na current is only ~25% of that of absorption. The Ca absorption rate is ~11% of that reported in Bindels et al. (1992). This value is reasonable, since Bindels' data is an aver-

TABLE III

Equilibrium Solution for Open-circuited Epithelium between Equal Ringer Solutions

	Mucosal	Cytoplasm	Serosal	
		mV		
ϕ	−37.1	−76.1	0.0	
		10^{-3} *cm³/cm² ep.*		
V		1.37		
		mM		
C^{i}_{k}				
Na	140.0	13.7	140.0	
K	5.0	140.2	5.0	
Cl	149.0	23.7	149.0	
Ca	2.0		2.0	
IMP	0.0	118.3	0.0	
OSM	296.0	296.00	296.0	
	C^{p}_{Ca}	CaB^{p}	C^{c}_{Ca}	CaB^{r}
		μM		
Ca	93.5×10^{-3}	1.7	34.4	488.8
J_k	mp	ps	ms	net
		pmol/s·cm² ep.		
Na	843.1	843.1	−246.6	596.5
K	−548.6	−548.6	−14.7	−563.3
Cl	0.02	0.02	35.0	35.0
Ca	1.2	1.2	−0.29	0.89
J_k	Na/K pump	Cotransporter	Ca pump	Na/Ca exchange
		pmol/s·cm² ep.		
Na	874.5	−26.0		−0.06
K	−583.0	−26.0		
Cl		−51.9		
Ca			1.16	0.02
ER flux	$V^{r} \cdot J^{tp}_{leak}$	$V^{r} \cdot J^{tp}_{ch}$	$V^{r} \cdot J^{pr}_{pump}$	
		pmol/s·cm² ep.		
	0.73	0.76	1.50	

age of the connecting tubule and that of the cortical collecting tubule. The Ca absorption rate in connecting duct is known to be significantly higher than that in the CCT (Costanzo and Windhager, 1992).

Closed-circuit epithelium. In the case of closed-circuit, electrical potential in the lumen and the bath are coupled together at ground potential. The mathematical description of the closed-circuit differs from the open circuit by having one less independent differential equation, since $\phi^{ps} = \phi^{pm}$ and $\phi^{ms} = 0$. The electrical current passing through the tight junction becomes zero, because of the parallel short circuit of zero resistance. We denote the membrane potential of the principal cell by ϕ^{p}. This membrane potential is determined by the combined fluxes of the cell from the apical and basolateral membrane, given in the following equation.

$$C_q^p \frac{d\phi^p}{dt} = -\sum_{k=1}^{4} z_i F(J_k^{pm} + J_k^{ps}) \qquad (22)$$

Table IV contains the steady state solution for the closed-circuit solution. The membrane potential of the principal cell is −56.1 mV, an intermediate value between ϕ^{ps} and ϕ^{pm} in the open circuit case. This change in the membrane potential gives an increased Ca influx from apical membrane, ending up with $C^p_{Ca} = 120$ nM, higher than 93.5 nM in the open-circuit case. The increase in C^p_{Ca} decreases the Na influx across the apical membrane. There is an increase in the electrochemical gradient for the entry of Na as ϕ^{pm} is increased. But this is not sufficient to offset the effect of C^p_{Ca} on the Na channel. As a result, the net Na transport across the apical membrane is decreased. This leads to a decrease in Na concentration in cytoplasm. Concurrently, K concentration is increased. Cytoplasmic Cl concentration also increases, because the basolateral membrane potential becomes less negative. Cell volume increases slightly as Cl enters the cell across the basolateral membrane.

TABLE IV

Equilibrium Solution for Closed-circuited Epithelium between Equal Ringer Solutions

	Mucosal	Cytoplasm	Serosal	
		mV		
ϕ	−56.1	−56.1	0.0	
		10^{-3} cm³/cm² ep.		
V		1.38		
		mM		
C_k^i				
Na	140.0	11.9	140.0	
K	5.0	141.7	5.0	
Cl	149.0	32.9	149.0	
Ca	2.0		2.0	
IMP	0.0	109.5	0.0	
OSM	296.0	296.0	296.0	
	C^p_{Ca}	CaB^p	C^r_{Ca}	CaB^r
		μM		
Ca	120.0×10^{-3}	2.12	38.70	523.5
J_k	mp	ps	ms	
		pmol/s·cm² ep.		
Na	766.0	766.0	0	
K	−289.4	−289.4	0	
Cl	0.063	0.063	0	
Ca	1.62	1.62	0	
J_k	Na/K pump	Cotransporter	Ca pump	Na/Ca exchange
		pmol/s·cm² ep.		
Na	790.5	−20.9		−0.61
K	−527.0	−20.9		
Cl		−41.8		
Ca			1.83	−0.20
ER flux	$V^r J^{rp}_{leak}$	$V^r J^{rp}_{ch}$	$V^r J^{pr}_{pump}$	
		pmol/s·cm² ep.		
	0.83	1.07	1.90	

Ca Dynamics in Open-Circuit Epithelium

Decreasing NaCl in the serosal medium. If Na/Ca exchange exists in the principal cells, manipulations in extracellular Na concentration should affect C^p_{Ca} dynamics. Bourdeau and Lau tested this idea by isosmotically replacing NaCl in the serosal solution with other nonpermeable species in the connecting tubule (Bourdeau and Lau, 1990).

The effect on C^p_{Ca} by decreasing NaCl in the serosal medium (Bourdeau and Lau, 1990) and numerical simulation of the same protocol are shown in Fig. 4. In the simulation, NaCl in the serosal medium is replaced by impermeant species (e.g., mannitol) at time 5–15 min, with a linear ramp of 1 min on each side. Final C^s_{NaCl} is 50, 30, 14, and 7 mM for the corresponding curves. Steady state C^p_{Ca} increases as C^s_{NaCl} is dropped. C^p_{Ca} shows an overshoot at the initial period of onset on decreasing C^s_{Na} both experimentally and numerically. This overshoot is caused by the kinetic characteristic of the Ca channels on the ER. Depending on how fast and the extent of C^s_{NaCl} changes, the overshoot can either return to the steady state monotonically ($C^s_{NaCl} = 50$ mM), or show damping oscillation and gradually return to the high level of state steady level ($C^s_{NaCl} = 14$ mM). It is interesting to see how these details of the experiment are captured by the simulation.

Cytoplasmic Ca increases little as Na concentration in the bathing medium drops 50 mM% from its background level of 140 mM. This means the principal cell can keep C^p_{Ca} at almost a constant level during physio-

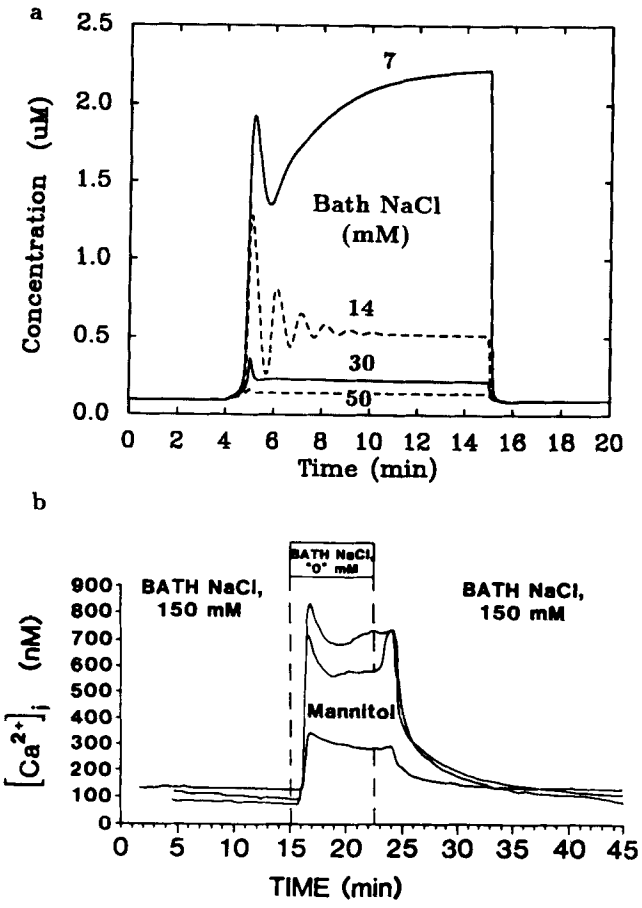

FIGURE 4. Effect on C^{P}_{Ca} of isosmotically decreasing NaCl in the bath. (*a*) Numerical simulation. Serosal NaCl is replaced by impermeant species (e.g., mannitol) at time 5–15 min, with a linear ramp of 1 min on each side. Final serosal NaCl is 50, 30, 14, and 7 mM. (*b*) Experimental result. Serosal NaCl is replaced by mannitol completely in three different experiments in the cortical connecting tubule. Data from Bourdeau and Lau (1990) with permission.

logical changes in C^{s}_{NaCl}. The increase in C^{P}_{Ca} becomes much more substantial, as C^{s}_{NaCl} falls below 20% of the physiological range. The initial Ca accumulation is caused by the reversal of Na/Ca exchange, transporting Ca into the cell (Fig. 2 *c*). This reversal in direction, however, does not necessarily hold for the behavior of the system at the steady state. As Ca accumulates in the cytoplasm, the apical Na entry is inhibited due to the effect of C^{P}_{Ca} on the apical Na channel. As a consequence, cytoplasmic Na level drops and the apical membrane hyperpolarizes. The hyperpolarization of apical membrane increases the apical entry of Ca, contributing to the secondary Ca accumulation. This secondary Ca accumulation, together with a decreased cytoplasmic Na level, decreases the Ca entry from the basolateral membrane via the Na/Ca exchanger, or even reverse its direction of Ca transport. At steady state, the sustained elevation of Ca is maintained mainly by increased Ca entry through the apical membrane.

Simulation with only C^{s}_{Na} decreased but not Cl shows a similar profile of C^{P}_{Ca}, in agreement with experimental observations (Bourdeau and Lau, 1990). If NaCl is decreased to 5 mM, C^{P}_{Ca} rises to a toxic level of ~8 μM. Further decrease of serosal NaCl leads to uncontrolled Ca increase; which is caused by the massive Ca entry from the apical membrane with a severely hyperpolarized potential and the almost complete annihilation of Na/Ca exchange. Under similar circumstance, experimental results show C^{P}_{Ca} stabilized in the μM range. This difference between the model and the experimental data can be explained by factors not included in the model. One possible mechanism is through the downregulation of apical Ca entry caused by saturation or other feedback regulations. The other

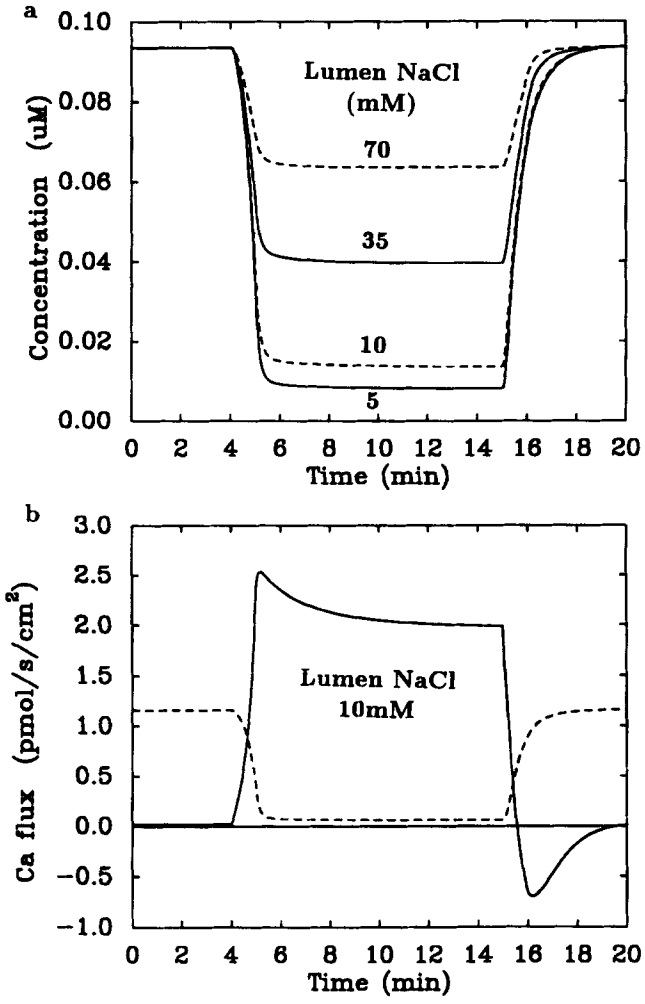

FIGURE 5. Effect on C^{P}_{Ca} of isosmotically decreasing NaCl in the lumen. In *a*, mucosal NaCl is replaced by impermeant species (e.g., mannitol) at time 5–15 min, with a ramp of 1 min on each side. Final mucosal NaCl concentrations are 70, 35, 10, and 5 mM. (*b*) Components of Ca fluxes across the basolateral membrane with mucosal NaCl at 10 mM; flux by Na/Ca exchange (*solid line*), by Ca-ATPase (*dashed line*).

is through the insertion of new Ca-ATPase into the basolateral membrane.

Decreasing NaCl in the luminal medium. Alternatively to decreasing C^{s}_{NaCl}, one can lower C^{m}_{NaCl} and observe its effect on C^{P}_{Ca}. Experimental results obtained by Bourdeau and Lau show that such a maneuver actually decreases C^{P}_{Ca}, i.e., its effect on C^{P}_{Ca} is the opposite of decreasing C^{s}_{NaCl} (Bourdeau and Lau, 1990).

Our numerical simulations behave similarly. In Fig. 5 *a* the numerical results are shown. NaCl in the lumen is isosmotically replaced by impermeant species as in Fig. 4 to different levels. Steady state C^{P}_{Ca} drops as C^{m}_{NaCl} is dropped. When C^{m}_{NaCl} is dropped by 50%, C^{P}_{Ca} drops from 93.5 nM to 63.7 nM. In the extreme case, when C^{m}_{NaCl} is 5 mM, C^{P}_{Ca} drops to a very low level of 8.1 nM. In experimental data, the drop of C^{P}_{Ca} is less substantial, even when C^{m}_{NaCl} is at 0. There are two possible reasons for this discrepancy: (*a*) the experimental dye (fura-2) is inaccurate for C^{P}_{Ca} below 100 nM; (*b*) low C^{P}_{Ca} might increase apical Ca conductance. Other possibilities of intracellular Ca regulation may be also involved.

As Na in the lumen drops, so does the Na flux into the cytoplasm from the apical surface. The Na/K pump in the basolateral membrane will still operate in the same mode as governed by Eq. 4, pushing the steady state C^{P}_{Na} downward. The decrease in C^{P}_{Na} alters the activity of Na/Ca exchange, making it more effective in transporting Ca out of the cell (Fig. 2 *a*). As more C^{P}_{Ca} is transported out of the cell than that enters, C^{P}_{Ca} decreases. In Fig. 5 *b* we show a typical case of the Ca fluxes across the basolateral membrane where C^{m}_{NaCl} is at 10 mM. The Ca outward flux carried by Na/Ca exchange increases from close to zero to a stable value of 2.0 pmol/s · cm² ep. This increase causes the drop in C^{P}_{Ca}, and the Ca flux carried by the Ca-ATPase decreases from 1.2 pmol/s · cm² ep. to 0.06 pmol/s · cm² ep. correspondingly. The decrease in Ca-ATPase activity can not completely compensate the net increase in Na/Ca exchange activity. The net increase in Ca outward current is about 0.7 pmol/s · cm² ep.

Several other events occur to up-regulate C^{P}_{Ca} under these circumstances, in addition to the downregulation of Ca-ATPase. One is the increase in apical Ca influx. This increase is induced by the increase in the Ca concentration gradient across the apical membrane. The other is the feedback regulation of Ca on the apical Na channel. As C^{P}_{Ca} drops, the Na channel conductance increases, according to Eq. 21. This increase in Na entry will offset the net decrease in C^{P}_{Na} induced by decreasing C^{m}_{NaCl}. This loop of interaction actually prevents the drop in C^{P}_{Na} and hence a drop in C^{P}_{Ca} through the action of Na/Ca exchange. The changes in membrane potentials also contribute to the upregulation of C^{P}_{Ca}, which will be detailed later. All of these

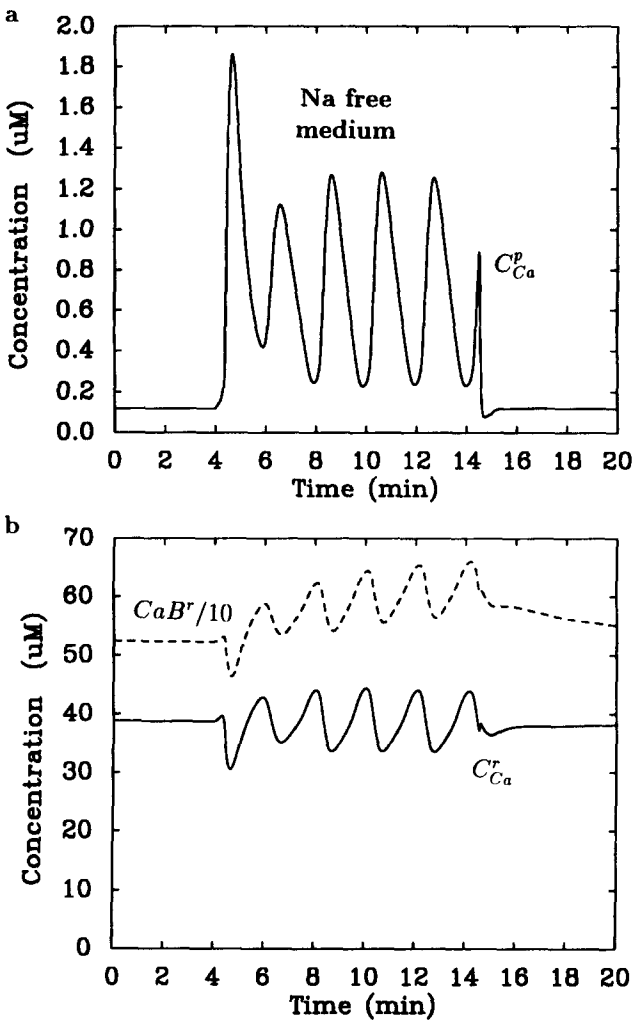

FIGURE 6. Ca oscillations of the principal cell in Na free medium. Extracellular NaCl is isosmotically replaced by impermeant species (e.g., TEA-Cl) from 140 to 0 mM in 4.5–14.5 min, with a linear ramp of 0.5 min from each end. Stable Ca oscillation is induced, as reported from experiments in Koster et al. (1993). (*a*) Ca in cytoplasm; (*b*) Ca inside ER (*solid line*) and buffered Ca inside ER (*dashed line*, scaled by a factor of 1/10).

regulations are feedback controls, induced by the primary action, and acting to diminish its final effect, but the net effect on the system will still be a decrease in C^{P}_{Ca}.

Ca Oscillations in the Closed-Circuit Epithelium

Koster et al. (1993) reported that in the cultured principal cell of CCT, C^{P}_{Ca} can show an oscillatory response, induced by lowering C^{o}_{Na} below 5 mM. The oscillation frequency is ~0.64/min and the peak is around 600 nM. Koster's experiment was done with cultured cells in a homogeneous medium, where the distinction between mucosal and serosal compartments no longer exists. The mathematical description of the cultured cell

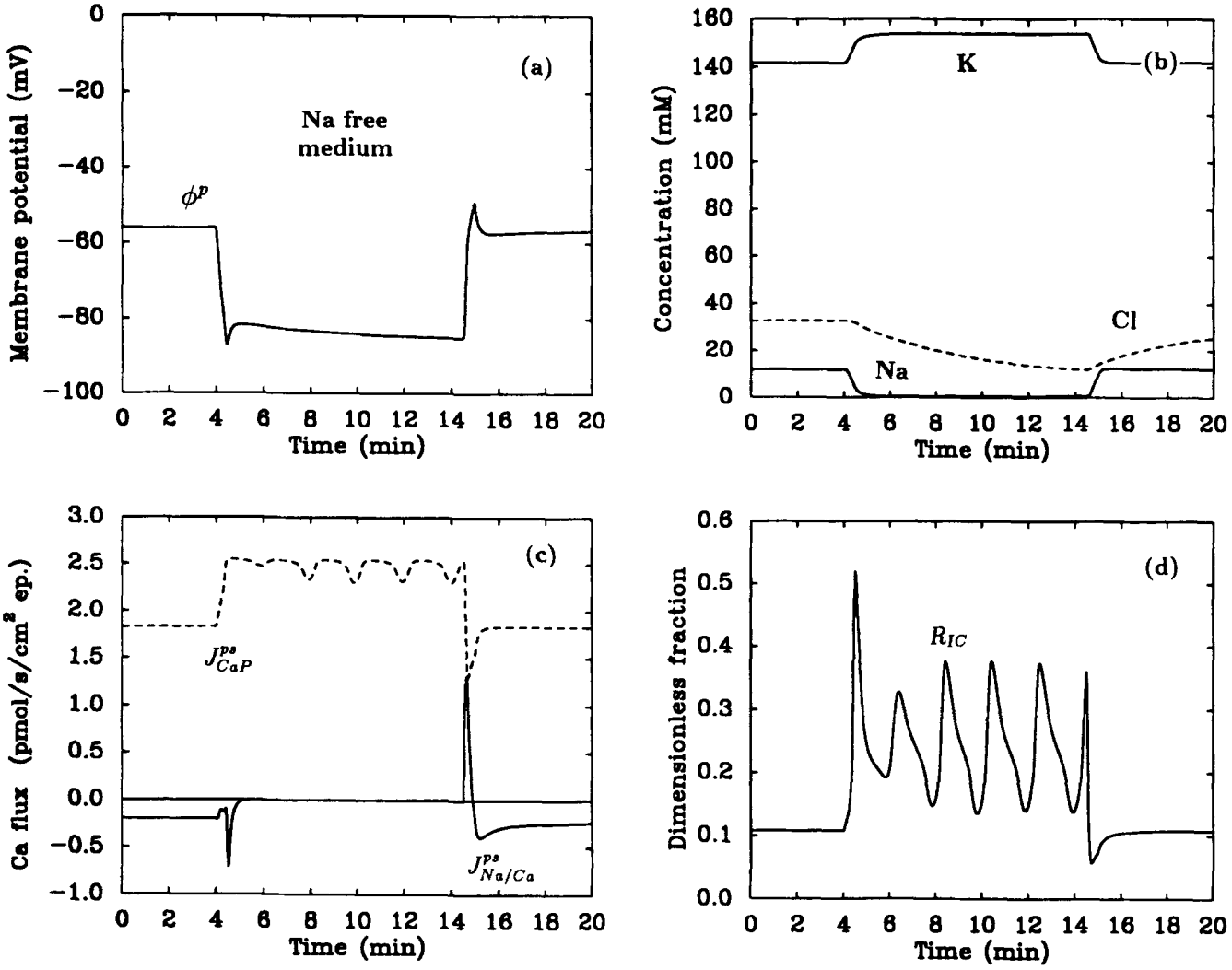

FIGURE 7. Other intracellular responses of the principal cell in Na-free medium. Extracellular Na profile is the same as in Fig. 6. (*a*) Membrane potential; (*b*) electrolyte concentrations; (*c*) Ca fluxes carried by Ca-ATPase and Na/Ca exchange; (*d*) fraction of the IP_3R channels in the activated (R_{IC}) state.

is actually the same as for the closed-circuit epithelium, since $\phi^{pm} = \phi^{ps}$, and the other components of the system in Eq. 20 are unchanged. The membrane potential of the principal cell (ϕ^p) is determined by the combined apical and basolateral membrane fluxes as in Eq. 22. As a principal cell is detached from the epithelium and put in a culture of the same ionic composition, apical Ca entry will increase substantially as the apical membrane becomes more hyperpolarized. To maintain a proper basal level of cytoplasmic Ca, the principal cell can either increase the amount of basolateral Ca-ATPase, or down-regulate the apical Ca-conductive channels. In the simulation, we increase the maximal basolateral Ca rate $P^{ps}_{max,Ca}$ from 1.9 pmol/s · cm² ep. to 2.55 pmol/s · cm² ep.

In the simulation, the decrease in C^o_{Na} is isoosmotically replaced by impermeant species coupled to Cl ion. As C^o_{Na} is completely replaced, C^p_{Ca} oscillation begins immediately (Fig. 6), and stabilizes after the first several spikes. Peak C^p_{Ca} is ~1.25 μM and frequency is about 0.5/min. The oscillation in C^p_{Ca} is also reflected in phase by the profile of CaB^p, C^r_{Ca}, and CaB^r (Fig. 6 *b*). There is excessive release from the ER when the oscillation begins, and excessive uptake of Ca as C^o_{Na} is restored (Fig. 6 *b*). In the cytoplasmic Ca profile, the first spike is substantially higher than the other spikes. As C^o_{Na} is restored, C^p_{Ca} shows a slight dip before it returns to its steady state, which is caused by reversal of Na/Ca exchange as C^o_{Na} is withdrawn (Fig. 7 *c*). Both of these features have been observed in experimental results (Fig. 1 in Koster et al., 1993).

The primary source for the periodic C^p_{Ca} increase is the periodic release from the internal Ca store, ER, not by periodic entry of Ca from extracellular medium. As

shown by Fig. 6 *b*, Ca released from the ER in a period is sufficient to explain the maximal C^{P}_{Ca} spike. The transient spiking is an internal characteristic of the cytoplasm-ER network, primarily caused by the biphasic property of the IP_3R. When C^{P}_{Ca} is low, C^{P}_{Ca} induces IP_3R to open, causing further Ca release from the ER (positive feedback); when C^{P}_{Ca} is high, it inhibits IP_3R from opening (negative feedback). From a kinetic point of view, the positive feedback loop has a faster time scale than that of the negative feedback loop. In a certain range of Ca in the cytoplasm-ER network, the positive feedback loop (Ca induces Ca release) and the negative feedback loop (Ca inhibits Ca release) work hand in hand to generate the oscillatory pattern. The contribution from a decreased C^{o}_{Na} is to increase the net amount of Ca in the ER-cytoplasmic network. As the total amount of Ca in the cytoplasm-ER network increases to a certain value, oscillation begins.

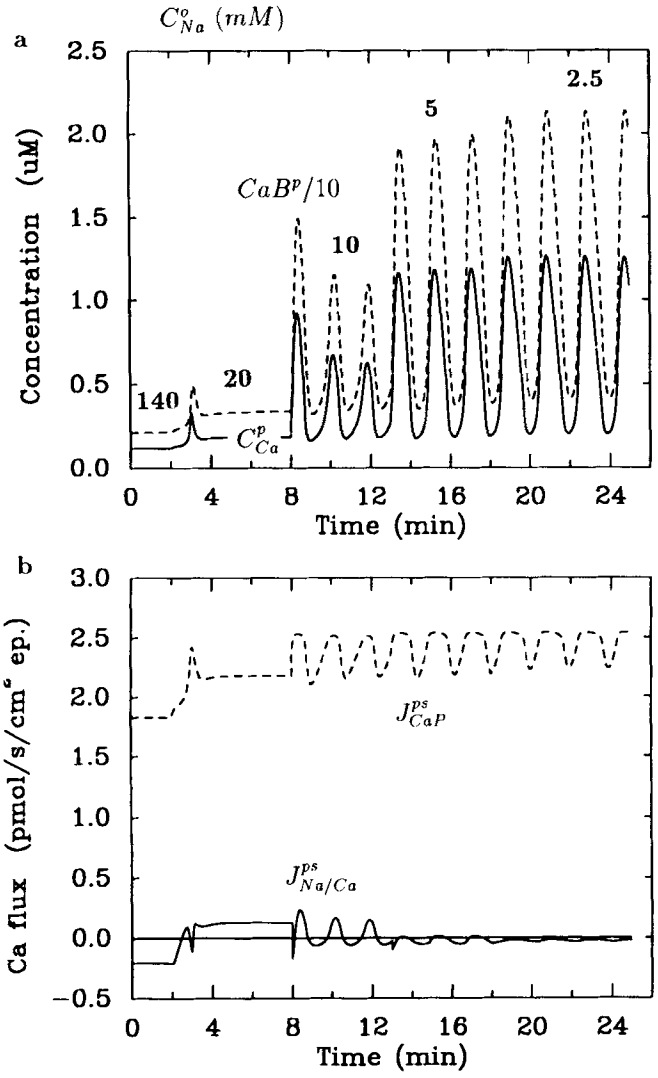

FIGURE 8. The effect of decreasing extracellular Na to different concentrations. Extracellular NaCl is replaced by TEA-Cl or choline-Cl from 140 to 20 mM linearly in 2–3 min; held at 20 mM in 3–8 min; and decreased further to 10 mM in 8–13 min, 5 mM in 13–18 min, and 2.5 mM in 18–25 min. (*a*) Free Ca (*solid line*) and buffered Ca (*dashed line*, scaled by a factor of 1/10) in the cytoplasm; (*b*) Ca fluxes carried by the Ca-ATPase (*dashed line*) and the Na/Ca exchange (*solid line*).

Fig. 7 shows the cellular events in Na free medium. When C^{o}_{Na} is dropped, membrane potential is hyperpolarized by more than 20 mV. This hyperpolarization is caused by the withdrawal of the sodium gradient across the membrane. Extracellular Ca enters the cell due to this hyperpolarization. This increase in Ca influx is the main source for the increased Ca in the cytoplasm-ER network that drives the Ca oscillation. A second source of initial Ca accumulation is through the Na/Ca exchanger. As C^{o}_{Na} is depleted, C^{P}_{Na} decreases to almost zero. These changes in the Na concentration across the cell membrane at first enhance Ca uptake by the cell through Na/Ca exchange ($C^{P}_{Na} > C^{o}_{Na}$). At steady state, however, Na/Ca exchange almost stops functioning because of the disappearance of the Na gradient. Compared with its earlier role of actively transporting Ca inwards, the inhibition of Na/Ca exchange actually decreases the net Ca accumulation inside the cell. Therefore, the contribution of the Na/Ca exchanger to the steady state intracellular Ca is, counter-intuitively, negative.

Although C^{P}_{Ca} regulates Na permeability in the apical portion of the membrane, we see no detectable potential fluctuations in Na free medium (Fig. 7 *a*). Since Na concentrations are zero in both intracellular and extracellular media, changes in Na conductance will not affect membrane potential. For other cellular responses, C^{P}_{K} increases from 142 to 153.8 mM; Cl leaves the cell slowly, causing cell volume to decrease slightly (result not shown).

As argued before, the kinetic properties of the IP_3R mandate C^{P}_{Ca} oscillation over a certain range of C^{o}_{Na}. In our model, Ca starts to oscillate when C^{o}_{Na} is below 10 mM, and continues until C^{o}_{Na} is zero. Fig. 8 shows C^{P}_{Ca} dynamics when C^{o}_{Na} is sequentially decreased. As C^{o}_{Na} first drops from 140 to 20 mM, C^{P}_{Ca} increases slightly from 120 nM to a steady state of 181 nM. The small spike within 2–4 min in front of the oscillations is typical and has been seen in Fig. 4. As C^{o}_{Na} reaches 10 mM, C^{P}_{Ca} shows oscillations with decreasing amplitude, which will eventually settle down to a stable oscillation with peak C^{P}_{Ca} level at 508 nM and at a frequency of 0.58/min. Further decrease in C^{o}_{Na} increases the oscillation amplitudes, as shown in Fig. 8 with C^{o}_{Na} = 5 mM in 13–18 min and with C^{o}_{Na} = 2.5 mM in 18–24 min. For C^{o}_{Na} = 5 mM, the oscillation frequency is 0.53/min and the amplitude 1.18 μM; for C^{o}_{Na} = 2.5 mM, the frequency is 0.51/min and the amplitude 1.25 μM. The oscillation frequency changes only slightly in the oscil-

lation range as C^{o}_{Na} changes, in agreement with experimental observations (Koster et al., 1993). There are, however, significant increases in the amplitude as C^{o}_{Na} decreases. When C^{o}_{Na} is fixed at below 10 mM, C^{p}_{Ca} oscillations are stable over time and return to the basal level between cycles. With the restoration of Na in the media, Ca oscillation disappears immediately.

C^{p}_{Ca} buffers bind to Ca quickly and oscillate in phase with C^{p}_{Ca} (Fig. 8 *a*). The buffered Ca in the cytoplasm is ~20 times the free Ca over all of the oscillatory phase. The cytoplasmic Ca buffers are not saturated as Ca oscillates; otherwise the linear correlation between free Ca and buffered Ca will be violated. For Ca oscillation to occur, the positive and negative feedback loops via IP_3R have to be triggered. Especially, free cytoplasmic Ca has to reach a certain critical value for the positive feedback loop to function. The buffered cytoplasmic Ca level has to reach its corresponding level, in the equilibrium of binding and unbinding with the free Ca. Since the buffered Ca represents the majority of Ca in cytoplasm, for Ca oscillation to occur, the amount of net Ca entry needed is determined mainly by the Ca buffering capacity in the cytoplasm and that inside the ER.

As C^{o}_{Na} is reduced, the Ca flux carried by the Na/Ca exchange varies. Since the function of the Na/Ca exchanger is determined by multiple factors, it is hard to

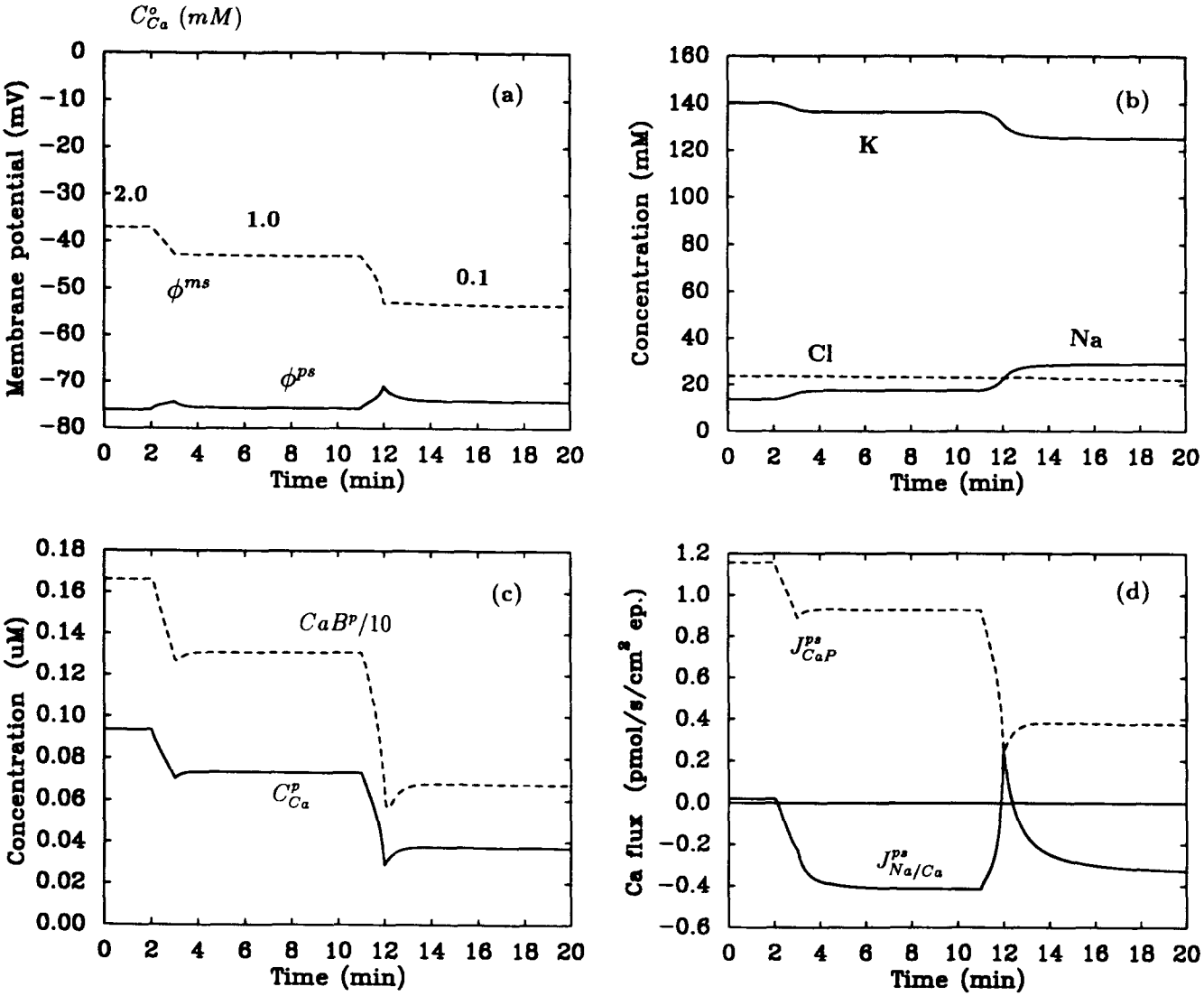

FIGURE 9. Response of the principal cell to decreasing extracellular Ca with feedback regulation. The feedback regulation of Ca on the apical Na permeability is responsible for maintaining intracellular Ca homeostasis. Ca in both the lumen and the bath are reduced sequentially from 2 mM (0–2 min) to 1 mM (3–11 min) and then to 0.1 mM (12–20 min), with 1 min ramp in each case. Membrane potentials and intracellular Na and K concentrations adjust slightly in response (*a* and *b*). Cell can retain a relatively high level of C^{p}_{Ca} even at very low extracellular Ca (0.1 mM) (*c*), due to the reversal of the Na/Ca exchange. (*d*) shows the components of J_{Ca} flux across the basolateral membrane.

predict which way the Ca flux will vary. The complex response pattern of the Na/Ca exchanger is shown in Fig. 8 *b*. Initially, the Na/Ca exchanger is transporting Ca inward to the cytoplasm. When C^{o}_{Na} is dropped to 10 mM, this flux becomes positive, i.e., transporting Ca out of cytoplasm. As C^{p}_{Ca} oscillates, Na/Ca exchange can show oscillatory changes in direction, as shown here in the 8–13-min region; or it can stay at the negative domain (for $C^{o}_{Na} < 2.5$). We can conclude here that Na/Ca exchange is not essential for the Ca oscillation; its role is secondary compared with the change in membrane potential. In addition, it is not necessary for Na/Ca exchange to alternate its direction during Ca oscillations. The basolateral Ca-ATPase activity is increased significantly as C^{o}_{Na} is dropped, mainly to pump out the extra Ca entry caused by the hyperpolarized membrane.

In the oscillatory mode, the basolateral Ca-ATPase operates at a close to maximal rate. Especially, it shows saturation at the peak of C^{p}_{Ca} spike. This saturation of the Ca-ATPase is one characteristic of Ca oscillations observed in the simulation. Because of the relative high density of the basolateral Ca-ATPase and a low basal level of cytoplasmic IP_3, the basolateral Ca-ATPase can equilibrate Ca release from ER through the IP_3R, thus maintaining an equilibrium cytoplasmic Ca at relatively higher levels, compared to other cell types where the Ca-ATPase is not present or at low levels. Therefore, for Ca oscillation to occur under this experimental protocol, the basolateral Ca-ATPase has to be partially saturated. It is, however, not a necessary condition for intracellular Ca oscillations under other experimental conditions, nor does it hold for other epithelial cell types. Many manipulations, such as blocking the basolateral Ca-ATPase, increasing IP_3 cytoplasmic Ca level, or changes on the ER Ca pump or membrane leakage,

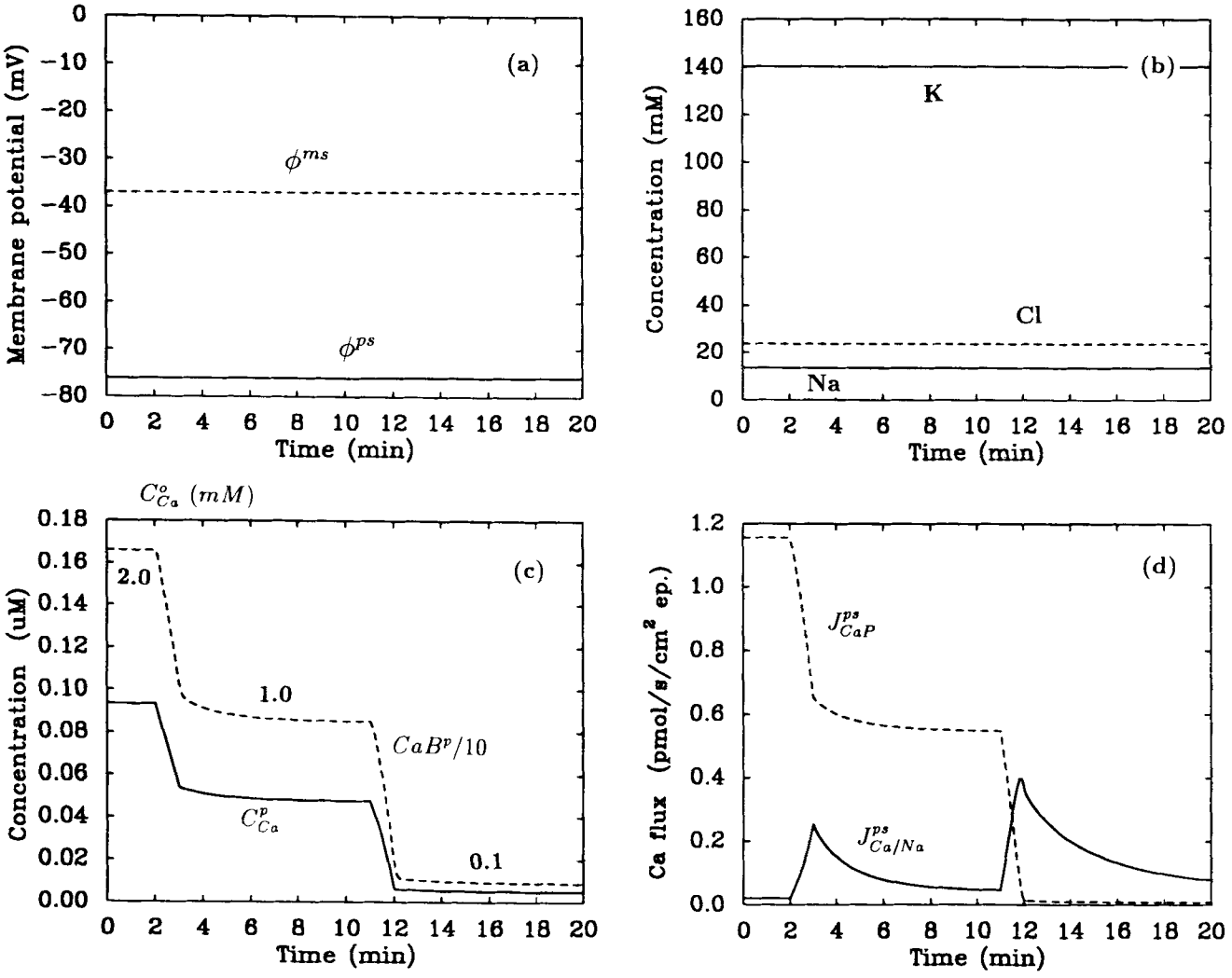

FIGURE 10. Response of the principal cell to decreasing extracellular Ca without feedback regulation. Extracellular Ca protocol is the same as in Fig. 9. The changes in membrane potentials and intracellular concentrations of Na, Cl, and K are not detectable (*a* and *b*). Cell has limited regulation of C^{p}_{Ca} as C^{o}_{Ca} drops (*c*). Na/Ca exchange cannot reverse its direction (*d*) (compare with Fig. 9 *d*).

can induce oscillations as well (results not shown). These oscillations do not involve the interplay of ionic species other than Ca, and they have been studied in many cell types by several groups of investigators (Keizer and De Young, 1993; Li et al., 1994; Tang and Othmer, 1994).

Regulation of Intracellular Ca by Na/Ca Exchange and Apical Ionic Channels

In this section, we will explore the regulation of intracellular Ca in the open-circuit epithelium, especially the processes mediated through Na/Ca exchange. We will show that intracellular Ca concentration is tightly regulated through the coupled effect of Na/Ca exchange on the basolateral membrane and the Ca regulated Na conductance on the apical membrane (Eq. 21). The cell, under extracellular Ca stress, can regulate cytoplasmic Ca concentration into the narrow region that is acceptable to life, by sacrificing a small variation in intracellular Na. In addition, this regulation of Ca on the apical Na channel can be replaced by the regulation of Ca on the apical K channel.

Decreasing extracellular Ca. If extracellular Ca is decreased, we would expect C^{P}_{Ca} to decrease. Experimental results and numerical simulations confirm this point (Bourdeau and Lau, 1990; Frindt et al., 1993). In Fig. 9, C^{o}_{Ca} (both lumen and bath) is first reduced from 2 to 1

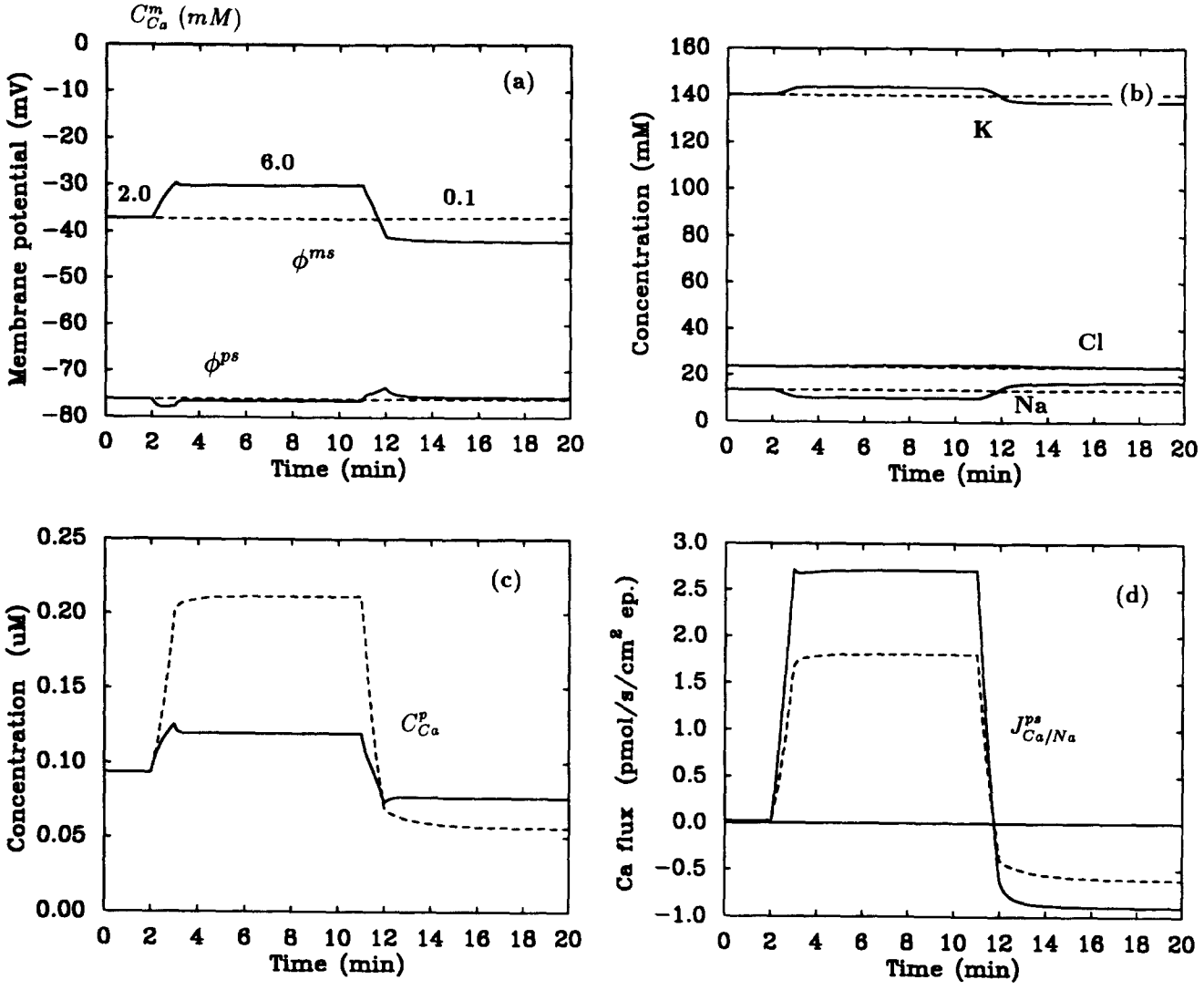

FIGURE 11. Responses of the principal cell to variations of Ca in the lumen with (*solid lines*) or without (*dashed lines*) the feedback regulation. Luminal Ca is held at 2 mM initially, increased to 6 mM within 3–11 min, and decreased to 0.1 mM in 12–20 min, with linear ramps of 1 min between each transition. The comparisons of membrane potentials are shown in (*a*), while that of Na and K in (*b*). C^{P}_{Ca} is controlled tightly with the feedback regulation compared with C^{P}_{Ca} without the regulation (*c*). The differences are caused by the different rates of the Na/Ca exchange in transport of Ca (*d*).

mM, and then to 0.1 mM. C^{p}_{Ca} drops correspondingly. The decrease in C^{p}_{Ca}, however, is not very severe; C^{p}_{Ca} is at a relatively high level of 37.4 nM even at 0.1 mM C^{o}_{Ca}. This is obtained by the reversal in the direction of Na/Ca exchange, which will be explored later. Na concentration becomes elevated and K concentration decreased. This is not surprising since a low C^{p}_{Ca} increases the apical Na conductance. Membrane potential across pm changes a little, and that across the epithelium more significantly; ϕ^{ms} becomes hyperpolarized as Na absorption rate across the epithelium increases. The absorption rate increases from 843 to 1,250 pmol/s · cm^2 ep. at 0.1 mM C^{o}_{Ca} (result not shown).

In Fig. 9 *d* we show the two components of Ca fluxes across the ps membrane, i.e., that due to Ca-ATPase and that due to Na/Ca exchange. As C^{o}_{Ca} is decreased from 2 to 1 mM, Na/Ca exchange immediately reverses its direction, transports a large flux of Ca back into the cell. This reversal of Ca flux maintains C^{p}_{Ca} at 73 nM. As C^{o}_{Ca} drops further, Na/Ca exchange first extrudes Ca and soon reverses its direction again. The first phase of this response, changing from inward transport to outward transport, is directly caused by a drop in C^{o}_{Ca} (see Fig. 2 *d*). As C^{p}_{Ca} decreases in response, however, the Na/Ca exchanger becomes inwardly transporting again, preventing the further loss of C^{p}_{Ca}. The final inward transport rate is a little smaller for C^{o}_{Ca} = 0.1 mM compared with that for 1 mM. From Fig. 2 *d*, one can see that C^{p}_{Ca}, like the Na/Ca exchanger, is controlled by a multitude of factors and its final value reflects a balance among them. The complexity in the homeostasis of C^{p}_{Ca} argues strongly for a quantitative model versus simple intuition.

In Fig. 10, simulation conditions are the same as in Fig. 9, except that the regulation of Ca on the apical Na channel is removed. Under this condition, the change of membrane potential is abolished as C^{o}_{Ca} is dropped, since no change in membrane conductance takes place (Fig. 9 *a*). Decreasing C^{p}_{Ca} by itself has negligible effect on ϕ^{pm}. As a result, changes in intracellular concentrations of Na, K, and Cl are undetectable (Fig. 9 *b*). The change in C^{p}_{Ca} is much more substantial compared with the case of Fig. 9. It decreases from 93.5 to 49.3 nM with 1.0 mM extracellular Ca; a further drop to 5 nM occurs when C^{o}_{Ca} is decreased to 0.1 mM (Fig. 9 *c*). At C^{o}_{Ca} = 0.1 mM, Ca in the ER is almost zero (result not shown).

Fig. 10 *d* provides an explanation for the significant low level of C^{p}_{Ca} at low extracellular Ca concentrations compared with that in Fig. 9 *c*. A drop in extracellular Ca actually increases the rate of Ca outward transport through the Na/Ca exchanger, because the Ca gradient across the basolateral membrane is smaller, and the Na gradient and membrane potential are unchanged. As C^{p}_{Ca} drops, this increased rate will decrease. The pumping rate of Ca pump also decreases significantly. These actions, however, are not sufficient to upregulate C^{p}_{Ca}. A sufficient regulation requires the reversal of Na/Ca exchange, but the mediator (C^{p}_{Na}) is not available here without the regulation of P^{pm}_{Na} by C^{p}_{Ca} (see Fig. 9 *d*).

Varying Ca in the lumen only. In the above study, as Ca in the serosal medium is decreased, it affects the driving force for Na/Ca exchange outside the cell. In the following case, we study the feedback regulation of C^{p}_{Ca} with Ca in the serosal medium fixed. Fig. 11 shows a simulation with only C^{m}_{Ca} being varied. A comparison is made with the feedback regulation of C^{p}_{Ca} on the apical Na channel (*solid lines*) and without the regulation (*dashed lines*). As one can see here, without the regulation of C^{p}_{Ca} on the apical Na permeability, cytoplasmic Ca varies dramatically as C^{m}_{Ca} varies. Feedback regulation reacts to counteract the effect, mainly by decreasing C^{p}_{Na} slightly. As is in the previous case, the change in C^{p}_{Na} is relatively small. The stable Na concentrations with C^{m}_{Ca} at 2.0 mM is 13.7 mM, decreased to 10.4 mM with 6 mM C^{m}_{Ca}, and increased to 16.9 mM with 0.1 mM C^{m}_{Ca}.

This slight change in C^{p}_{Na} has a profound effect on C^{p}_{Ca}, as demonstrated in Fig. 11 *c*. Without the feedback regulation, C^{p}_{Ca} would be increased to 211.5 nM with C^{m}_{Ca} = 6 mM, and decreased to 56.1 nM with

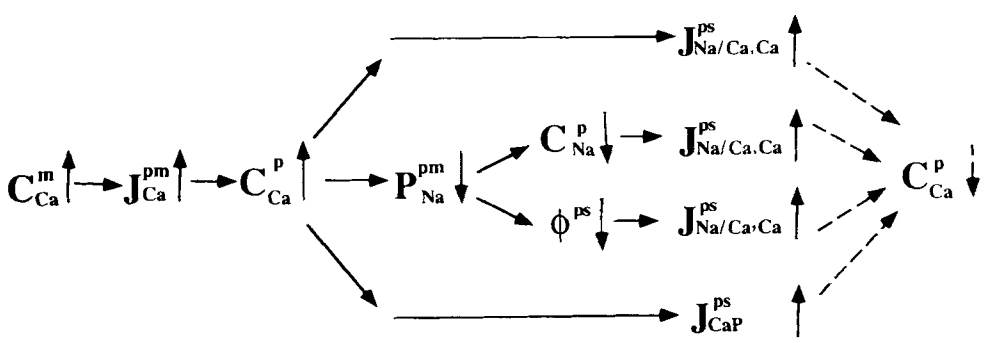

FIGURE 12. Different feedback regulation pathways in regulating cytoplasmic Ca as luminal Ca is increased. The main contributors, that mediated through the feedback regulation of Ca on the apical Na conductance, are shown in the middle. A slight decrease in cytoplasmic Na concentration has a profound effect on the Na/Ca exchange in maintaining intracellular Ca.

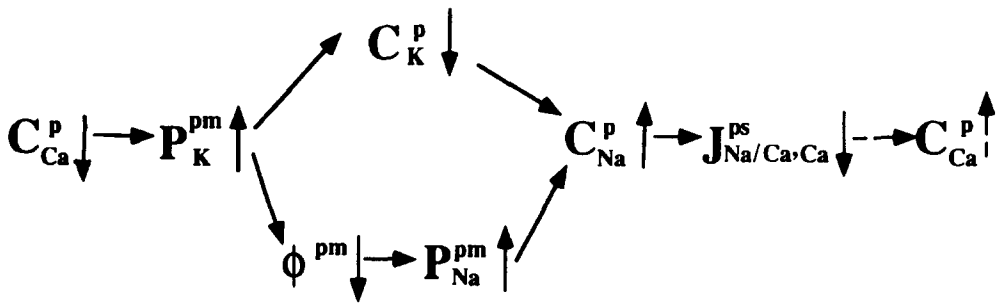

FIGURE 13. An alternative route of feedback regulations in maintaining Ca homeostasis in the principal cell. In this route, cytoplasmic Ca does not regulate the apical Na permeability directly. Instead, it regulates the apical K permeability, as suggested in Wang et al. (1993). When cytoplasmic Ca decreases, more K is secreted through the apical membrane, inducing an increase in cytoplasmic Na due to the electroneutrality condition of the cytoplasm. In addition, the apical membrane becomes hyperpolarized, causing an increase in the apical Na permeability, as suggested by Frindt et al. (1993). Increased cytoplasmic Na affects the Na/Ca exchange to upregulate cytoplasmic Ca.

C^{m}_{Ca} = 0.1 mM. With the slight change of C^{p}_{Na}, the corresponding C^{p}_{Ca} variations are much less intensive, increasing only to 119.6 nM with C^{m}_{Ca} = 6 mM, and decreasing to 76.3 nM with C^{m}_{Ca} = 0.1 mM. The change of Ca in the ER is similar to that of Ca in cytoplasm. As C^{m}_{Ca} is varied between 0.1 to 6 mM, the ER store of Ca varies from 21.8 to 41.0 μM without the feedback regulation. This differs significantly from the case where the regulation is present, where C^{r}_{Ca} varies from 29.7 to 38.7 μM (result not shown).

The significant effect of slight changes in C^{p}_{Na} on C^{p}_{Ca} is mediated through the Na/Ca exchange, the dynamics of which is shown in Fig. 11 *d*. At the steady state of C^{m}_{Ca} = 2 mM, Na/Ca exchange is essentially nonfunctional. But as soon as C^{p}_{Ca} departs from its equilibrium value of 93.5 nM, Na/Ca exchange starts to function. It can work in either of the two directions, positively or negatively, to down regulate the change in C^{p}_{Ca}. The down regulation is substantially potentiated with the introduction of a feedback regulation of cell Na. The cell here sacrifices a small variation in C^{p}_{Na} to obtain the homeostasis of the very important intracellular signal species, C^{p}_{Ca}. Because of the stoichiometry of the Na/Ca exchange (3 Na for 1 Ca), a slight change in C^{p}_{Na} can induce profound change in the rate of Na/Ca exchange. Mathematically speaking, the variation in C^{p}_{Na} is raised to its third power to affect the exchange. Hence a small change in C^{p}_{Na} induces a magnified response.

The pathway for the feedback regulation of C^{p}_{Ca} is shown in Fig. 12. As C^{m}_{Ca} increases, the Ca flux across the apical membrane, J^{pm}_{Ca}, increases. This increase breaks the previous balance between Ca entry and Ca exodus. C^{p}_{Ca} increases. The increase in C^{p}_{Ca} triggers three different types of feedback regulation. The first is the increased pumping of Ca through the Ca pump (J^{ps}_{CaP}). The second is the increased transporting of Ca through Na/Ca exchange as C^{p}_{Ca} increases. These two feedback regulations only involve the basolateral membrane. The third, the most important, is the regulation mediated through P^{pm}_{Na}. As C^{p}_{Ca} increases, the permeability of the apical Na channel, P^{pm}_{Ca} decreases (Frindt and Windhager, 1990). This triggers two events: (*a*) the basolateral membrane potential, ϕ^{ps}, becomes slightly hyperpolarized; (*b*) C^{p}_{Na} drops slightly. The slight hyperpolarization of the basolateral membrane has the effect of increasing the rate of Na/Ca exchange in transporting Ca outward (Fig. 2). More importantly, the slight drop in C^{p}_{Na} induces a significant change in the rate of Na/Ca exchange, to counterbalance the change in C^{p}_{Ca}, as shown in Fig. 11 *d*.

The regulation of C^{p}_{Ca} when C^{v}_{Ca} is decreased is analogous to the above case, i.e., reversing the direction of all the arrows in Fig. 12. However, the feedback regulation of C^{p}_{Ca} on apical Na permeability is still controversial. Frindt et al. (1993) show evidence that the apical Na channel does not increase its open probability directly in response to a decrease in C^{p}_{Ca}. Instead, its open probability increases in response to the hyperpolarization of the apical membrane. This raises the question as to how the principal cell can upregulate C^{p}_{Ca} under severe decreases in extracellular Ca, as shown in Bourdeau and Lau (1990). One alternative explanation exists. That is to assume that Ca regulates the apical K channel. Wang et al. (1993) show that cytoplasmic Ca affects P^{pm}_{K} significantly. As C^{p}_{Ca} is increased from 125 to 335 nM, the K permeability is reduced to a quarter of its previous value. Further increases in C^{p}_{Ca} induce further inhibition in the K channel. If one assumes that this trend of regulation is continued as C^{p}_{Ca} is in the range of below 100 nM, then this feedback regulation pathway will effectively upregulate C^{p}_{Ca} as C^{m}_{Ca} drops.

The inhibition of apical K permeability by C^{p}_{Ca} will induce a similar feedback regulation of Ca as demonstrated earlier. As C^{p}_{Ca} decreases, P^{pm}_{K} will increase, causing a decrease in C^{p}_{K} (note $C^{p}_{K} > C^{m}_{K}$); C^{p}_{Na} in turn increases as more Na enters the cell in response to a hyperpolarized apical membrane. Thus the cytoplasm remains electrically neutral (similarly, as C^{p}_{Na} increases in response to decrease in C^{m}_{Ca} in Fig. 11 *b*, C^{p}_{K} de-

creases). The increase in C^{p}_{Ca} then mediates its effect through the reversal of the Na/Ca exchange, similar to the case in Fig. 11. In our computer simulation, we use a similar profile of Ca regulation of P^{pm}_{K} as in Fig. 3, except that the decaying rates of the exponentials are doubled.

$$P^{pm}_{K} = \begin{cases} 0.9P^{pm}_{K,0}\exp^{-28\,(C_{Ca}-K_{K,Ca})\times 10^{3}} + 0.1\,P^{pm}_{K,0} \\ \qquad \text{if } C_{Ca} < K_{K,Ca} \\ 0.9P^{pm}_{K,0}\exp^{-8.048\,(C_{Ca}-K_{K,Ca})\times 10^{3}} + 0.1\,P^{pm}_{K,0} \end{cases} \tag{23}$$

otherwise, where $P^{pm}_{K,0}$ is the P^{pm}_{K} value given in Table I, and $K_{K,Ca}$ is 93.5 nM, the equilibrium value for the open circuit. The simulation results are similar to those in Figs. 9 and 11, and are omitted here.

In addition, as P^{pm}_{K} increases, the apical membrane become hyperpolarized significantly (~11 mV as C^{m}_{Ca} = 0.1 mM, result not shown). If P^{pm}_{Na} is responsive to membrane potentials, as suggested in Frindt et al. (1993), this will introduce an additional pathway to upregulate the decrease in C^{p}_{Ca}. As the apical membrane becomes hyperpolarized, the open probability of apical Na channels increases significantly. This will lead to an increase in C^{p}_{Na}, hence a stronger effect of Na/Ca exchange. Qualitatively, the regulation of C^{p}_{Ca} on apical K permeability has the same effect as on apical Na permeability. But computer simulation shows that regulation of Na permeability is more effective quantitatively in maintaining Ca homeostasis. This insufficiency in upregulation through K permeability alone may be compensated by the regulation of the apical Na channel by ϕ^{pm}. In this way, the regulation of C^{p}_{Ca} is mediated through the combined effects of Ca-sensitive apical K channels, and the potential-sensitive apical Na channel (see Fig. 13). In addition, the net entry of Na across the apical membrane also increases in response to a steeper membrane gradient.

For the principal cell, all of the above-mentioned processes may be at work, providing ample safeguards against external perturbation of C^{p}_{Ca}. All of these feedback regulations tend to increase the cytoplasmic Na concentration when C^{p}_{Ca} drops. The end effect, the upregulation of C^{p}_{Ca}, is achieved most effectively.

Experimental evidence shows that change in extracellular Ca concentration alone has very little effect on C^{p}_{Ca} (Bourdeau and Lau, 1990). We believe that is due to the feedback regulations presented above. Simple experiments can be designed to check the mechanism proposed here. As extracellular Ca (or Ca in the lumen) is changed, one could measure the transepithelial membrane potential ϕ^{ms} and C^{p}_{Ca} simultaneously. The above simulations predict significant changes in transepithelial potential if either one of the feedback regulations via the apical membrane is present, while the change in C^{p}_{Ca} should be relatively small.

DISCUSSION

We have proposed a simplified model of the epithelium for the cortical collecting tubule, consisting of a population of the principal cells joined by tight junctions. Detailed components of Ca dynamics are introduced, including Na/Ca exchange and Ca-ATPase on the basolateral membrane, the IP_3R Ca channels on the ER membrane, and Ca buffering inside the cytoplasm and the ER. Our model is the first to incorporate realistic Ca dynamics in a computational model for epithelial cells. The scheme developed here can be applied to modeling Ca dynamics in other epithelial cell types.

The model requires some type of Cl cotransport mechanism at either the apical or the basolateral membrane in order to explain the experimentally observed C^{p}_{Cl} concentration. Through computer simulation of the model, the experimental observations on C^{p}_{Ca} caused by varying Na concentrations in the serosal and luminal compartments are reproduced. Specifically, decreasing Na in the serosal medium increases C^{p}_{Ca}; whereas decreasing Na in mucosal medium decreases C^{p}_{Ca}. For cultured principal cells, the model predicts Ca oscillation when C^{o}_{Na} is below 10 mM. This model can be used to further study Ca mediated regulation of Na and K transport in the cortical collecting duct.

Experimental evidence for the existence of an apical Ca channel in the principal cells is secondary. The observed large Ca absorption rate in Bindels et al. (1992) can only be explained by a channel-mediated process. Their results, however, are obtained from the cultured cell, not from the principal cell in vivo. Ling et al. report the identification of an amiloride-insensitive nonselective cation channel in the apical surface (Ling et al., 1991). This channel could be responsible for the Ca conductance. In this paper, we do not include a specific Ca channel in the apical membrane. On the other hand, we permit quite a large Ca current across the apical membrane through a nonspecific conducting mechanism. This nonspecific conductance generates a Ca reabsorption rate in the order of 1 pmol/s · cm^2 ep., which is much less than the value of 20 pmol/s · cm^2 ep. reported in Bindels et al. (1992). Ca reabsorption through the tight junction is of the same order but quantitatively smaller. In vivo experiments suggest no significant Ca absorption across the principal cells. Ca absorption might be through the tight junction by a diffusional mechanism, and determined only by the electrochemical gradient of Ca across the epithelium (Bourdeau and Hellstorm-Stein, 1982). This issue needs to be clarified by further experimental research.

The kinetic model by Hoffman and Tosteson (1971) we used for the Na/K pump does not include the voltage-dependence of the pump; thus its use is restricted to cases with only small variations of the basolateral membrane potential around its equilibrium value. All the simulations in this paper approximately satisfy this condition, but it can be violated under certain experimental procedures such as the application of ouabain (Silver et al., 1993). The exact electrogenic nature of the pump is still being explored experimentally (Hilgemann, 1994); however, there appears to be sufficient data to warrant a more detailed kinetic model, which would account for the electrogenic steps in the transporting cycle. The thermodynamic model we used for the Na:K:2Cl cotransporter is also an approximation, which shows no saturation of ionic binding and would fail if the concentration of an ionic species becomes exactly zero. Saturation of ionic binding is unlikely to occur in the simulated experimental procedures, since K, Na, and Cl are either in the range of physiological values or lower than that. For the simulation of Na free serosal medium, serosal Na is linearly ramped down over time to a small number so that the ratio of cytoplasmic Na to Na in the serosal medium remains bounded. Models of thermodynamic type are first-order linear approximations to the biochemical nonlinearities. To better represent the biochemical process of the cotransporter, a kinetic model based on experimental data is needed (Miyamoto et al., 1986; Haas, 1994). This effort is currently underway.

Ca Oscillations

Since the cytoplasmic IP_3 is at the fixed basal level, the Ca oscillation in the ER-cytoplasmic system of the principal cell is not induced by an increase in IP_3, but by an increase of total amount of Ca in the ER-cytoplasm system. As the total amount of Ca in the ER-cytoplasmic Ca increases, C^{P}_{Ca} increases. At a critical level of C^{P}_{Ca}, the positive feedback loop of calcium induced calcium release through IP_3R is triggered, followed by the slower process of the negative feedback loop, i.e., the inhibitory effect of Ca on IP_3R. Thus the cell Ca becomes oscillatory. This type of oscillation has also been seen in the mathematical models for the pancreatic β cell. As the clamped voltage varies, the entry Ca flux across plasma membrane changes. The cytoplasmic Ca oscillates as the entry Ca flux exceeds a certain level, and the the oscillation frequency and amplitude also depend on the magnitude of this flux (Keizer and De Young, 1993). In a mathematical model for the cardiac myocytes with ryanodine-sensitive intracellular Ca channels, the cytoplasmic Ca becomes oscillatory as membrane Ca leakage increases. The effect of the increased leakage is to increase the total amount of Ca in the ER-cytoplasm complex (Tang and Othmer, 1994).

In our simulations, oscillation can arise in the principal cell through changing Na in the serosal medium only (result not shown), or Na in both serosal and mucosal media as shown in this paper. In this case, the increased Ca influx is mainly caused by the hyperpolarization of the apical membrane as extracellular Na is removed. The role of Na/Ca exchanger is only secondary. At the initial phase of decreased extracellular Na, it contributes to the Ca accumulation as intracellular Ca is low. In the later and steady state phase, as cytoplasmic Ca increases and the cytoplasmic Na decreases, the role of the Na/Ca exchanger is not necessarily transporting Ca inward, as shown in Figs. 7 and 8. It can actually enhance the Ca-ATPase in transport Ca out of the cell. This complex behavior of the Na/Ca exchanger in response to a drop in extracellular Na is counter-intuitive and can only be captured through detailed quantitative modeling efforts.

Experimental observations on oscillatory responses by the principal cell are reported only in Koster et al. (1993), which are cultured principal cells instead of in cells in intact epithelium. Spontaneous Ca oscillations have also been observed in Madin-Darby canine kidney cells transformed by alkaline stress (Wojnowski et al., 1994*a*,*b*). There, the oscillation of Ca is accompanied by membrane hyperpolarization, suggesting the activation of membrane K channels or the inhibition of Na channels or both are involved in the oscillations (Westphale et al., 1992; Wunsch et al., 1995). However, the Madin-Darby canine kidney cells are genetically transformed and do not have certain characteristics of epithelial cells. The excitable C^{P}_{Ca} dynamics reported in Hebert et al. (1990); Champingeulle et al. (1993); and Naruse et al. (1991) serve as an indirect confirmation of oscillations in intact epithelium. The lack of experimental observations on oscillation in epithelium may be due to difficulties in determining C^{P}_{Ca} for individual cells. The experimental measurement of Ca for a population of cells can average out C^{P}_{Ca} oscillations that are not in phase with each other, giving the deceptive impression of a uniform increase in these cells of C^{P}_{Ca} with large superposed noise (Koster et al., 1993).

The Role of Na/Ca Exchange and Ca Regulated Na and K Permeability in Ca Homeostasis

According to our simulations, the role of Na/Ca exchange in Ca reabsorption is very limited. Compared with the Ca transport by the Ca-ATPase, Na/Ca exchange only carries 1.7% of transepithelial Ca flux at the steady state. In the normal range of Na and Ca in the cytoplasm and serosal medium, the flux due to the Na/Ca exchange is close to zero; the major portion of Ca reabsorption by the epithelium is carried by the Ca-ATPase.

The role of Na/Ca exchange appears not to be for Ca reabsorption, but for intracellular Ca homeostasis. If C^{P}_{Ca} departs from normal physiological values, no matter for what reason, the cell attempts to counter the change via Na/Ca exchange both directly and indirectly. Directly, an increase of C^{P}_{Ca} will increase the rate of $J^{pm}_{Na/Ca,Ca}$. Since the Ca-ATPase has a K_M of ~0.1 μM (Gmaj and Murer, 1988), it is saturated at C^{P}_{Ca} higher than 0.5 μM. In these cases, Na/Ca exchange takes over from the Ca-ATPase as the main mechanism for Ca extrusion. Since Na/Ca exchange does not saturate over the μM range of C^{P}_{Ca} (Fig. 2 *c*), it can protect the cell from the toxic effect of very high C^{P}_{Ca}. On the other hand, if C^{P}_{Ca} becomes very low, Na/Ca exchange can reverse its direction and transport Ca into the cytoplasm from the serosal medium. In this circumstance, it counteracts the effect of Ca-ATPase by bringing extracellular Ca into the cell.

The indirect regulation of the Na/Ca exchanger on C^{P}_{Ca} is mediated through cytoplasmic Na. An increase in C^{P}_{Ca} will downregulate the apical Na entry through Ca-sensitive Na channels, decrease C^{P}_{Na}, and hyperpolarize the basolateral membrane slightly. All these changes will increase the efficiency of Na/Ca exchange in transporting Ca outward. Alternatively, C^{P}_{Ca} can regulate the apical K channel. Either way, the cell sacrifices a small change in C^{P}_{Na} to restore C^{P}_{Ca} at a relatively low value. Because of the 3:1 stoichiometry of the Na/Ca exchange, only a slight change in C^{P}_{Na} is needed to boost the Na/Ca exchange rate significantly for effective Ca regulation.

If the main role of the Na/Ca exchange is for intracellular Ca homeostasis through either direct or indirect pathways, Na/Ca exchange should stay close to its electrochemical stationary state, i.e., $J^{Ca}_{Na/Ca} = 0$, during normal physiological status of the cell; because in this state, the Na/Ca exchange is most sensitive to changes in C^{P}_{Ca} and C^{P}_{Na} in either direction. In addition, no free energy is dissipated by the exchange when cytoplasmic Ca is at its normal value.

The direct and indirect effect of Na/Ca exchange on Ca homeostasis may be employed in other cell types where Na/Ca exchange has been found and where large Ca influx from extracellular medium is needed, for example, in the cardiac myocytes. Theoretically, it is reasonable for different cell types to have different stoichiometries of Na/Ca exchange, since the stoichiometry should be tuned to fit the special intracellular and extracellular environments of the specific cell type. Indeed, in the retinal photoreceptors of rods and cones, the Na/Ca exchange has a stoichiometry other than 3Na:1Ca. It is actually a Na/Ca,K exchange with the stoichiometry of 4Na:1K:1Ca (Yau, 1994). The higher coupling ratio between Ca and Na and the additional coupling of cotransport between Ca and K could be a reflection of the extra-sensitiveness of these cells to Ca variations. Whatever is the case, the quantitative study of cellular models similar to the model we have developed for the principal cell of CCT may help to decipher the role of Na/Ca exchange in a variety of cell types.

We thank Drs. G. F. Frindt, L. G. Palmer, A. M. Weinstein, and E. E. Windhager for their helpful discussions during the development of this model. This work is supported by National Institutes of Health grant DK31550.

Original version received 26 April 1995 and accepted version received 19 October 1995.

REFERENCES

Abercrombie, R., and N. Al-Baldawi. 1990. Ca^{2+} binding by *Myxicola* neurofilament proteins. *Cell Calcium.* 11:361–370.

Al-Baldawi, N., and R. Abercrombie. 1990. Properties of calcium binding by *Mmyxicola* neurofilament protein. *Cell Calcium.* 11: 459–467.

Al-Baldawi, N., and R. Abercrombie. 1995. Cytoplasmic calcium buffer capacity determined with Nitr-5 and DM-nitrophen. *Cell Calcium.* 17:409–421.

Atri, A., J. Amundson, D. Clapham, and J. Sneyd. 1993. A single-pool model for intracellular calcium oscillations and waves in the *Xenopus* laevis oocyte. *Biophys. J.* 65:1727–1739.

Bezprozvanny, I., and B. Ehrlich. 1994. Inositol (1,4,5)-trisphosphate ($InsP_3$)-gated Ca channels from cerebellum: Conduction properties for divalent cations and regulation by intraluminal calcium. *J. Gen. Physiol.* 104:821–856.

Bindels, R., P. Ramakers, J. Dempster, A. Hartog, and C. van Os. 1992. Role of Na^+/Ca^{2+} exchange in transcellular Ca^{2+} transport across primary cultures of rabbit kidney collecting system. *Eur. J. Physiol.* 420:566–572.

Borke, J., J. Minami, A. Verma, J. Penniston, and R. Kumar. 1987. Monoclonal antibodies to human erythrocyte membrane Ca^{2+}-Mg^{2+} adenosine triphosphatase pump recognize an epitope in the basolateral membrane of human kidney distal tubule cells. *J. Clin. Invest.* 80:1225–1231.

Bourdeau, J., and R. Hellstorm-Stein. 1982. Voltage-dependent calcium movement across the cortical collecting duct. *Am. J. Physiol.* 242:F285–292.

Bourdeau, J., and K. Lau. 1990. Basolateral cell membrane Ca-Na exchanger in single rabbit connecting tubules. *Am. J. Physiol.* 258: F1497–1503.

Bourdeau, J., A. Taylor, and A. Iacopino. 1993. Immunocytochemical localization of sodium-calcium exchange in canine nephron. *J. Am. Soc. Nephrol.* 4:105–110.

Campbell, D., W. Giles, K. Robinson, and E. Shibata. 1988. Studies of the sodium-calcium exchanger in bull-frog atrial myocytes. *J. Physiol.* 403:317–340.

Champingeulle, A., E. Siga, G. Vassent, and M. Imbert-Teboul. 1993. V_2-like vasopressin receptor mobilizes intracellular Ca^{2+} in rat medullary collecting tubules. *Am. J. Physiol.* 265:F35–45.

Chase, H., and Q. Al-Awqati. 1983. Calcium reduces the sodium permeability of luminal membrane vesicles from toad bladder. *J. Gen. Physiol.* 81:643–665.

Costanzo, L., and E. Windhager. 1992. Renal regulation of calcium balance. *In* The Kidney. D. Seldin, and G. Giebisch, editors. Raven press, NY. 2375–2394.

De Young, G., and J. Keizer. 1992. A single-pool inositol 1,4,5-trisphophate-receptor-based model for agonist-stimulated oscillations in Ca^{+2} concentration. *Proc. Natl. Acad. Sci. USA.* 89:9895–9899.

Doucet, A., and A. Katz. 1982. High-affinity Ca-Mg-ATPase along the rabbit nephron. *Am. J. Physiol.* 242:F346–352.

Frindt, G., and E. Windhager. 1990. Ca^{2+}-dependent inhibition of sodium transport in rabbit cortical collecting tubules. *Am. J. Physiol.* 258:F568–F582.

Frindt, G., R. Silver, E. Windhager, and L. Palmer. 1993. Feedback regulation of Na channels in rat CCT II. Effects of inhibition of Na entry. *Am. J. Physiol.* 264:F565–F574.

Garay, R., and P. Garrahan. 1973. The interaction of sodium and potassium with sodium pump in red cells. *J. Physiol.* 231:297–325.

Gmaj, P., and H. Murer. 1988. Calcium transport mechanisms in epithelial cell membranes. *Miner. Electrolyte Metab.* 14:22–30.

Goldman, D. 1943. Potential, impedance, and rectification in membranes. *J. Gen. Physiol.* 27:37–60.

Haas, M. 1994. The Na-K-Cl cotransporters. *Am. J. Physiol.* 267: C869–C885.

Haynes, D., and A. Mandveno. 1987. Computer modeling Ca^{2+} pump function of Ca^{2+}-Mg^{2+}-ATPase of sarcoplasmic reticulum. *Physiol. Rev.* 67:244–284.

Hebert, R., D. Fredin, H. Jacobson, and M. Breyer, 1990. PGE_2 inhibits AVP induced water flow in cortical collecting ducts by protein kinase C activation. *Am. J. Physiol.* 259:F318–F325.

Hilgemann, D. W. 1994. Channel-like function of the Na,K pump probed at microsecond resolution in giant membrane patches. *Science (Wash. DC).* 263:1429–1432.

Hindmarsh, A. 1974. GEAR: Ordinary Differential Equations System Solver. Lawrence Livermore Laboratory. Revision 3. Livermore, CA.

Hirsch, J., J. Leipziger, U. Frobe, and E. Schlatter. 1993. Regulation and possible physiological role of the Ca^{2+}-dependent K^+ channel of cortical collecting ducts of the rat. *Eur. J. Physiol.* 422:492–498.

Hoffman, J., and D. Tosteson. 1971. Active sodium and potassium transport in high potassium and low potassium sheep red cells. *J. Gen. Physiol.* 58:438–466.

Keizer, J., and G. De Young. 1993. Effect of voltage-gated plasma membrane Ca^{2+} fluxes on IP_3-linked Ca^{2+} oscillations. *Cell Calcium.* 14:397–410.

Kendall J., M. Badminton, and A. Campbell. 1994. Changes in free calcium in the endoplasmic reticulum of living cells detected using targeted aequorin. *Ann. Biochem.* 221:173-181.

Koster, H., C. van Os, and R. Bindels. 1993. Ca^{2+} oscillations in the rabbit renal cortical collecting system induced by Na^+ free solutions. *Kidney Int.* 43:828–836.

Li, Y., J. Rinzel, J. Keizer, and S. Stojilkovic. 1994. Calcium oscillations in pituitary gonadotrophs: comparison of experiment and theory. *Proc. Natl. Acad. Sci. USA.* 91:58–62.

Ling, B., D. Eaton, and C. Hinton. 1991. Amiloride-sensitive sodium channels in rabbit cortical collecting tubule primary cultures. *Am. J. Physiol.* 261:F933–F944.

Luo, C., and Y. Rudy. 1994. A dynamics model of the cardiac ventricular action potential I. Simulations of ionic currents and concentration changes. *Circ. Res.* 74:1071–1096.

Magaldi, A., A. van Baak, and A. Rocha. 1989. Calcium transport across rat inner medullary collecting duct perfused in vitro. *Am. J. Physiol.* 257:F738–F745.

Milner, R., K. Famulski, and M. Michalak. 1992. Calcium binding proteins in the sarcoplasmic/endoplasmic reticulum of muscle and nonmuscle cells. *Mol. Cell. Biochem.* 112:1–13.

Miyamoto, H., T. Ikehara, H. Yamaguchi, K. Hosokawa, T. Yonezu, and T. Masuya. 1986. Kinetic mechanism of Na^+, K^+, Cl^--cotransport as studied by Rb^+ influx into HeLa cells: effects of extracellular monovalent ions. *J. Memb. Biol.* 92:135–150.

Moore, L., D. Fitzpatrick, T. Chen, and E. Landon. 1974. Calcium pump activity of the renal plasma membrane and renal microsomes. *Biochim. Biophys. Acta.* 345:405–418.

Naruse, M., S. Uchida, E. Ogata, and K. Korokawa. 1991. Endothelin 1 increases cell calcium in mouse collecting tubule cells. *Am. J. Physiol.* 261:F720–F725.

Othmer, H., and Y. Tang. 1993. Oscillations and waves in a model of calcium dynamics. *In* Experimental and Theoretical Advances in Biological Pattern Formation. H. Othmer, J. Murray, and P. Maini, editors. Plenum Press, London. 295–319.

Palmer, L., and G. Frindt. 1987. Effects of cell Ca and pH on Na channels from rat cortical collecting tubule. *Am. J. Physiol.* 253: F333–339.

Parys, J., H. Smedt, P. Vandenberghe, and R. Borghgraef. 1985. Characterization of ATP-driven calcium uptake in renal basolateral and renal endoplasmic reticulum membrane vesicles. *Cell Calcium.* 6:413–429.

Rick, R. 1993. Ion concentration changes in renal cells during regulatory volume decrease. *Am. J. Physiol.* 265:F77–F86.

Robertson, S., J. Johnson, and J. Potter. 1987. The time-course of Ca^{2+} exchange with calmodulin, troponin, parvalbumin, and myosin in response to transient increases in Ca^{2+}. *Biophys. J.* 34:559–569.

Schlatter, E., M. Bleich, J. Hirsch, U. Markstahler, U. Frobe, and R. Greger. 1993. Cation specificity and pharmacological properties of the Ca^{2+}-dependent K channel of rat cortical collecting ducts. *Eur. J. Physiol.* 422:481–491.

Schultz, S. 1980. Basic Principales of Membrane Transport. Cambridge Univ. Press, Cambridge.

Silver, R., G. Frindt, E. Windhager, and L. Palmer. 1993. Feedback regulation of Na channels in rat CCT I. Effect of inhibition of Na pump. *Am. J. Physiol.* 264:F557–F564.

Strieter, J., J. Stephenson, L. Palmer, and A. Weinstein. 1990. Volume-activated chloride permeability can mediate cell volume regulation in a mathematical model of a tight epithelium. *J. Gen. Physiol.* 96:319–344.

Strieter, J., J. Stephenson, G. Giebisch, and A. Weinstein. 1992*a*. A mathematical model of the rabbit cortical collecting tubule. *Am. J. Physiol.* 263:F1063–F1075.

Strieter, J., A. Weinstein, G. Giebisch, and J. Stephenson. 1992*b*. Regulation of K transport in a mathematical model of the cortical collecting tubule. *Am. J. Physiol.* 263:F1076–F1086.

Tang, Y. 1993. Theoretical Studies on Second Messenger Dynamics. University Microfilms Inc., Ann Arbor, MI. 266 pp.

Tang, Y., and H. Othmer. 1994. A model of calcium dynamics in cardiac myocytes based on the kinetics of ryanodine-sensitive calcium channels. *Biophys. J.* 67:2223–2235.

Tang, Y., and H. Othmer. 1995. Frequency encoding in excitable

systems and its application to calcium oscillations. *Proc. Natl. Acad. Sci. USA.* 92:7869–7873.

Tang, Y., J. Stephenson, and H. Othmer. 1996. Simplification and analysis of models calcium dynamics based on the kinetics of IP_3-sensitive calcium channels. *Biophys. J.* 70:246–263.

Wagner, J., and J. Keizer. 1994. Effects of rapid buffers on Ca^{2+} diffusion and Ca^{2+} oscillations. *Biophys. J.* 67:447–456.

Wang, W., J. Geibel, and G. Giebisch. 1993. Mechanism of apical K^+ channel modulation in principal renal tubule cells. *J. Gen. Physiol.* 101:673–694.

Watras, J., I. Bezprozvanny, and B. Ehrlich. 1991. Inositol 1,4,5-trisphoshate-gated channels in cerebellum: presence of multiple conductance states. *J. Neurosci.* 11(10):3239–3245.

Westphale, H., L. Wojnowski, A. Schwab, and H. Oberleithner. 1992. Spontaneous membrane potential oscillations in Madin-Darby canine kidney cells transformed by alkaline stress. *Eur. J. Physiol.* 421:218–223.

Windhager, E., G. Frindt, and S. Milovanovic. 1991. The role of Na-Ca exchange in renal epithelia. *Ann. NY Acad. Sci.* 639:577–591.

Wojnowski, L., J. Hoyland, W. Mason, A. Schwab, and H. Westphale. 1994*a*. Cell transformation induces a cytoplasmic Ca^{2+} oscillator in Madin-Darby canine kidney cells. *Eur. J. Physiol.* 426: 89–94.

Wojnowski, L., A. Schwab, J. Hoyland, W. Mason, and S. Silbernagl. 1994*b*. Cytoplasmic Ca^{2+} determines the rate of Ca^{2+} entry into Madin-Darby canine kidney-focus (MDCK-F) cells. *Eur. J. Physiol.* 426:95–100.

Wunsch, S., M. Gekle, U. Kersting, B. Schuricht, and H. Oberleithner. 1995. Phenotypically and karyotypically distinct Madin-Darby canine kidney cell clones respond differently to alkaline stress. *J. Cell Physiol.* 164:164–171.

Yamamoto-Hino, M., T. Sugiyama, K. Hikichi, M. Mattei, K. Hasegawa, S. Sekine, K. Sakurada, A. Miyawaki, T. Furuichi, M. Hasegawa, and K. Mikoshiba. 1994. Cloning and characterization of human type 2 and type 3 inositol 1,4,5-trisphosphate receptors. *Recept. Channels.* 2:9–22.

Yau, K. 1994. Phototransduction mechanism in retinal rods and cones. *Invest. Ophthalmol. & Visual Sci.* 35:9–32.

Zhou, Z., and E. Neher. 1993. Mobile and immobile calcium buffers in bovine adrenal chromaffin cells. *J. Physiol.* 469:245–273.